The mRNA export adaptor Yra1 contributes to DNA double-strand break repair through its C-box domain

*Valentina Infantino, *Evelina Tutucci♮, Noël Yeh Martin•, Audrey Zihlmann, Varinia García-Molinero, Géraldine Silvano, Benoit Palancade#, and Françoise Stutz+.

Dept. of Cell Biology, 30 Quai E. Ansermet, University of Geneva, 1211 Geneva, Switzerland.

♮ Department of Anatomy and Structural Biology, Albert Einstein College of Medicine, Bronx, NY 10461, USA

• Centre for Integrative Biology (CIBIO), University of Trento, Via Sommarive 9, 38123 Povo (TN), Italy.

Institut Jacques Monod, CNRS, UMR 7592, Univ Paris Diderot, Sorbonne Paris Cité, 15 rue Hélène Brion, 75013 Paris, France.

*Equal contribution

+ Corresponding author: Francoise.Stutz@unige.ch

ABSTRACT (168 words)

Yra1 is an mRNA export adaptor involved in mRNA biogenesis and export in *S. cerevisiae*. Yra1 overexpression was recently shown to promote accumulation of DNA:RNA hybrids favoring DNA double strand breaks (DSB), cell senescence and telomere shortening, via an unknown mechanism. Yra1 was also identified at an HO-induced DSB and Yra1 depletion causes defects in DSB repair. Previous work from our laboratory showed that Yra1 ubiquitination by Tom1 is important for mRNA export. Interestingly, we found that Yra1 is also ubiquitinated by the SUMO-targeted ubiquitin ligases Slx5-Slx8 implicated in the interaction of irreparable DSB with nuclear pores. Here we show that Yra1 binds an HO-induced irreparable DSB. Importantly, a Yra1 mutant lacking the evolutionarily conserved C-box is not recruited to an HO-induced irreparable DSB and becomes lethal under DSB induction in a HO-cut reparable system. Together, the data provide evidence that Yra1 plays a crucial role in DSB repair via homologous recombination. Unexpectedly, while the Yra1 C-box is essential, Yra1 sumoylation and/or ubiquitination are dispensable in this process.

Keywords: Yra1, HO endonuclease cut, genome instability, DSB repair, homologous recombination.

INTRODUCTION

Yra1 (Yeast RNA annealing protein 1) is an essential protein in *S. cerevisiae*, well characterized as an mRNA export adaptor involved in transcription elongation, 3' processing, and finally mRNA export together with the Mex67/Mtr2 export receptor and the poly(A) binding protein Nab2 (1).

Yra1 is evolutionarily conserved from yeast to human and belongs to the RNA and Export Factor (REF) family of hnRNP-like proteins (2-5). REF proteins include a conserved domain organization with a central RNP-motif containing an RNA binding domain (RBD) and two highly conserved N- and C-terminal boxes (N-box and C-box). These domains are separated by two variable regions (N-var and C-var), rich in positively charged amino acids that mediate interaction with RNAs and Mex67 (3, 6). *yra1* mutants lacking the RBD, the N-terminal or C-terminal (N-box+N-var or C-box+C-var) regions are viable indicating functional redundancy in their RNA binding properties. However, at least one highly conserved N-box or C-box is required for viability as deletion of both is lethal (7).

While Mex67 and Nab2 are shuttling between the nucleus and cytoplasm, Yra1 is a strictly nuclear protein (3, 5). Nuclear localization of Yra1 is important for mRNA export as mutants lacking the N-terminal nuclear localization signal (NLS) demonstrate nuclear accumulation of poly(A)+ RNA when examined by fluorescent *in situ* hybridization (FISH) (7). Yra1 binding to mRNA is important as well, as *yra1* mutants lacking the N- or C-terminal variable RNA binding domains also present poly(A)+ RNA export defects.

48 Interestingly, *yra1* mutants lacking the RBD also show some poly(A)+ RNA
49 export defect although this domain is not implicated in Mex67 interaction nor
50 RNA binding *in vitro*, suggesting that it may contribute to Yra1 function by
51 ensuring optimal folding of the protein. Loss of the highly conserved Yra1 C-
52 box (*yra1(1-210)* mutant) does not cause an obvious poly(A)+ mRNA export
53 defect, but it is required for optimal growth (7). This observation is consistent
54 with the fact that the C-box does not play a major role in Mex67 or RNA
55 binding and suggests that this highly conserved 16 amino acids sequence
56 may be important for another aspect of Yra1 function.

57 Different layers of regulations have been shown to modulate Yra1 levels
58 and function in mRNA biogenesis. We have previously shown that Yra1
59 ubiquitination by the E3 ligase Tom1 displaces Yra1 from messenger
60 ribonucleoparticles (mRNPs) as a quality control signal for correctly processed
61 mRNP prior to export into the cytoplasm (8). Another important feature for Yra1
62 regulation is that the *YRA1* gene harbors the second largest intron (776 nt) in
63 the *S. cerevisiae* genome, containing a non-canonical branchpoint sequence
64 (BS, gACUAAC) after a long first exon (300 nt). An excess of Yra1 protein
65 prevents *YRA1* pre-mRNA splicing and promotes export of the unspliced
66 transcript into the cytoplasm where it is degraded by the 5' to 3' decay pathway
67 (4, 9). It has been reported previously that the *yra1Δintron* mutant shows Yra1
68 protein overexpression (7) that is toxic for cell growth (10, 11) and impairs
69 poly(A)+ RNA export (12, 13). The presence of the *YRA1* intron is important to
70 maintain optimal Yra1 protein levels through Yra1 auto-regulation at the level
71 of splicing in a negative feedback mechanism (4). Studies on the *YRA1* gene
72 revealed that a mutation restoring a canonical branch-point sequence in the

73 context of the C-terminal mutation *yra1-F223S* or the C-terminal deletion *yra1-*
74 *ΔC11* is not viable. Overall, these mutagenesis experiments indicated that at
75 least three elements contribute to optimal Yra1 autoregulation: a long first
76 exon, a long intron, a weak branchpoint and an intact C-terminal domain (4).
77 The C-terminal domain was proposed to negatively regulate splicing provided
78 that splicing efficiency was suboptimal.

79 Independent studies have also indicated that besides its function in
80 mRNA biogenesis and export, Yra1 could contribute to DNA metabolism. It was
81 initially proposed that Yra1 interacts with a subunit of the DNA polymerase δ
82 and Dia2, an E3 ubiquitin ligase involved in DNA replication, genome stability
83 and S phase checkpoint recovery (14, 15). The C-box domain of Yra1 was
84 suggested to be necessary for the recruitment of Dia2 at replication origins
85 (15), establishing a potential functional link between Yra1 and DNA
86 metabolism. Another report provided evidence that strong Yra1 overexpression
87 causes transcription-associated hyper-recombination, a cell senescence-like
88 phenotype and telomere shortening, probably by counteracting telomere
89 replication since overexpressed Yra1 was located at the Y telomeric regions by
90 ChIP-chip. In the proposed model, Yra1 overexpression stabilizes R-loops,
91 which contain DNA:RNA hybrids and displaced DNA strands, favoring conflicts
92 between the replication fork and RNA Pol II resulting in genome instability (16,
93 17). Finally, a recent study based on ChAP-MS (chromatin affinity purification
94 with mass spectrometry) identified Yra1 in association with a reparable double-
95 strand break (DSB); moreover, a *yra1* DAmP (Decreased Abundance by mRNA
96 Perturbation) hypomorph mutant showed sensitivity to DSB agents and global
97 defects in DSB repair by pulse field gel electrophoresis (18).

98 DSBs can be repaired by two independent pathways: non-homologous
99 end joining (NHEJ) that joins the DNA ends of the lesion in an error-prone
100 process, and homologous recombination (HR), an error-free pathway used
101 when homologous DNA sequences are available for the repair (19). The genetic
102 instability resulting from unrepaired DSBs leads to cell death (20). The HR
103 process has to be tightly regulated to avoid aberrant genomic rearrangements.
104 On site sumoylation of HR proteins induced under DNA damage is pivotal to
105 ensure efficient and optimal DSB repair (21-24). SUMO-targeted E3 ubiquitin
106 ligases (STUbL), such as the Slx5-Slx8 complex in yeast, have also been
107 shown to contribute to the maintenance of genome stability, although their
108 targets have not been systematically identified (25).
109 In this work, we show that Yra1 is sumoylated by the SUMO ligases Siz1
110 and Siz2, desumoylated by the SUMO protease Ulp1 and ubiquitinated by the
111 SUMO-dependent E3 ligases Slx5-Slx8, which are important for genome
112 integrity (25, 26). Importantly, we find that Yra1 is recruited to DSBs and identify
113 the Yra1 C-box domain to be crucial for the binding and repair; however, Yra1
114 ubiquitination and/or sumoylation are not required in this process. Our results
115 strengthen the importance of Yra1 in genome integrity and provide evidence for
116 a critical role of Yra1 in DSB repair.
117

118 **MATERIALS AND METHODS**

119 **Yeast strains and plasmids**

120 The strains and plasmids used in this study are listed in Supplementary
121 Tables 1 and 2 (S1 and S2 Table). Primers are listed in Supplementary Table
122 3 (S3 Table).

123 The *YRA1* shuffled strains were obtained by transformation of the *YRA1*
124 shuffle strain (*yra1::HIS3*, YCpLac33-URA3-*YRA1*WT, Cen) with YCpLac22-
125 TRP centromeric plasmids encoding wild-type HA-tagged Yra1. The
126 transformed strains were plated on 5-FOA to select against the WT *YRA1*
127 URA3 plasmid. The cells able to grow on 5-FOA contain only the YCplac22-
128 TRP1-HA-*YRA1* WT plasmid (*YRA1* shuffled background). Single clones were
129 analyzed for correct auxotrophic markers and checked for HA-Yra1
130 expression by Western blot with αHA antibodies.

131 The strains with integrated WT or mutant *HA-YRA1* were obtained by
132 transformation of the W303 Mat-a/α diploid strain or FSY5073 (GA-6844 HO
133 irreparable system (27)) with a fragment containing the HA-tagged wild-type
134 or mutant *YRA1* sequences obtained by SmaI digestion of an engineered
135 pUC18 construct. The pUC18 plasmids were obtained by Gibson assembly
136 and contain a SmaI fragment consisting of the HA-tagged wild-type or mutant
137 *YRA1* sequences preceded by the *YRA1* promoter and followed by the *YRA1*
138 3' UTR, a selective marker (URA3 or HIS3) and an additional 100 pb of *YRA1*
139 3' downstream sequences. Yeast transformants were plated on the relevant
140 selective medium. Correct recombination and integration into the endogenous
141 *YRA1* locus was checked by PCR with a forward primer complementary to a
142 sequence -600bp upstream of the *YRA1* locus (OFS3118), not present in the

143 plasmid sequence, and a reverse primer matching the HA-tag sequence
144 present only in the plasmid-derived sequence (OFS3120). The W303 diploid
145 strains containing the integrated *HA-YRA1 WT* or *HA-yra1* mutant sequences
146 were sporulated on K-acetate agar plates for 3 days at 25°C and dissected.
147 Single spores were analyzed for relevant auxotrophic markers; HA-*YRA1*
148 integration was confirmed by PCR as described above and expression of HA-
149 Yra1 proteins was verified by Western blot.
150 The deletion strains were generated by homologous recombination of a
151 cassette containing an auxotrophic marker flanked by sequences adjacent to
152 the gene to delete. The pUG73::*LEU2,* pAG25::natMX4 or pUG6::kanMX6
153 cassettes were amplified by PCR using 80 nucleotides long forward and
154 reverse primers (20 nt complementary to the plasmid and 60 nt
155 complementary to the target sequences). PCR products were transformed
156 into the *YRA1* shuffle or WT W303 Mat-a/α diploid strains and correct
157 insertion confirmed by PCR. The W303 Mat-a/α diploid strains containing the
158 gene deletion were sporulated and single spores analyzed for auxotrophic
159 markers. Haploid Mat-α WT W303 deletion mutants were crossed with haploid
160 Mat-a strains containing integrated HA-YRA1 WT or mutant sequences
161 obtained as described above. The diploid *yra1* double mutants were
162 sporulated to obtain haploid *yra1* double mutants in W303 background. In the
163 case of deletions in the *YRA1* shuffle, the *yra1* double mutants were obtained
164 by plasmid shuffling as explained above.
165 The strains with integrated *HA-YRA1* in FSY6881 (NA17 strain with HO
166 reparable system) (28) were obtained after four back crosses between the
167 integrated *HA-YRA1 WT* or *HA-yra1(1-210)* and *HA-yra1allKR* mutants in

168 W303 and the NA17 strain. The sporulation, dissection and analysis of the
169 strains was performed as described above. The presence of the cassette
170 KanMX::HO-cs at URA3 and KanMX::ClaI at LYS2 was checked by PCR
171 followed by digestion with the restriction enzymes BamH1 (near the HO site)
172 and ClaI.

173 **Media and culture conditions**

174 If not specified, yeast strains were thawed on yeast extract-peptone-dextrose
175 (YPD) plates and grown for two days at 25°C. Cells were pre-cultured in 5 ml
176 of liquid YPD to reach an OD_{600}= 0.7-0.8 at 25°C and diluted into 100 ml YPD
177 overnight culture to reach OD_{600}= 0.8-1 at 25°C in the morning.
178 For the protein stability assays using metabolic depletion of *GAL-HA-YRA1* in
179 presence of the endogenous wild-type *YRA1* gene, cells expressing HA-Yra1
180 from the GAL promoter on a centromeric plasmid were grown over-night in
181 selective medium containing 2% galactose. When reaching OD_{600}=0.3, cells
182 were shifted to selective medium containing 2% glucose to repress *GAL-HA-*
183 *YRA1* and collected at time 0, 1h, 2h, 3h, 4h, 5h, 6h, and 7h following glucose
184 addition.
185 To induce the HO endonuclease-mediated irreparable DSB, cells were grown
186 over-night in SCLGg (SC lactate 2%/glycerol 2% containing 0.05% Glucose).
187 Cells at OD_{600}=0.4 were shifted to SCLGg medium containing 2% glucose for
188 2h (no cut induction) or to SCLGg medium containing 2% galactose to induce
189 the HO endonuclease. Cells were collected at 30 minutes, 1h, 2h and 4h
190 following galactose addition.
191 To induce the HO endonuclease-mediated reparable DSB, cells were grown
192 over-night in SCLGg (SC lactate 2%/glycerol 2% containing 0.05% Glucose).

193 Exponentially growing cells were treated with 2% galactose to induce the HO
194 endonuclease or not (control) for 2h. Serial dilutions of 200/100/50 cells were
195 plated on SCLGg Glu 2%. In another related experiment, serial dilutions of
196 exponentially growing cells in SCLGg medium were directly plated on SCLGg
197 Gal 2% or SCLGg Gal 3%-Raf 1% to induce the HO cut, and on SCLGg Glu
198 2% to repress HO endonuclease expression.

199 **Spot test**

200 Cells grown in YPD medium to stationary phase were diluted to OD_{600}=1 and
201 five 10-fold serial dilutions were prepared for spotting on agar plates. For each
202 spot, 3µl were deposited on 2% glucose YPD plates in the presence or
203 absence of drug (Zeocin 25 µg/ml, 50 µg/ml, and 100 µg/ml). Plates were
204 incubated at 25°C, 30°C, 34°C or 37°C for 3 days.

205 **Protein extraction and Western blotting**

206 Cells were grown to OD_{600}=1. Cell lysis was performed by adding 1 ml H_2O
207 with 150µl of Yex-lysis buffer (1.85M NaOH, 7.5% 2-mercaptoethanol) to the
208 pellet of 5 ODs of cells and kept 10 minutes on ice. Proteins were precipitated
209 by addition of 150µl of TCA 50% for 10 minutes on ice. The pellet was
210 resuspended in 30µl of 1X sample buffer (1M Tris-HCl pH6.8, 8 M Urea, 20%
211 SDS, 0.5M EDTA, 1% 2-mercaptoethanol, 0.05% bromophenol blue). Total
212 protein extracts were fractioned on SDS-PAGE and examined by Western
213 blotting with αHA (Enzo), αYra1 (Stutz laboratory), αPgk1 (Abcam), αRfa1, 2,
214 3 to detect RPA (kind gift from Vincent Géli), αGFP (Roche), αRad51 (Abcam)
215 antibodies. For quantitative Western blot analyses, fluorescent secondary α-
216 Mouse (IRDye 800CW) and α-Rabbit (IRDye 680RD) antibodies were used.
217 The signals were revealed with the LI-COR instrument.

218 **Chromatin immunoprecipitation (ChIP) and quantitative real-time PCR**

219 Cells grown to OD_{600}=1 were cross-linked with 1.2% of formaldehyde
220 (Molecular Biology grade Calbiochem™) for 10 minutes at 25°C under
221 continuous gentle agitation, quenched with 250mM of glycine (Sigma) for 5
222 min at 25°C and then on ice for at least 5 min, washed with PBS 1X and
223 frozen at -20°C. Pellets of 100 ml cultures at OD_{600}=1 were resuspended in
224 1ml of FA lysis buffer (10mM HEPES KOH pH 7.5, 140mM NaCl, 1mM EDTA
225 pH 8, 1%Triton X-100, 0.1% sodium deoxycholate) containing a protease
226 inhibitor cocktail (cOmplete tablets, Mini EDTA-free, Roche). Cells were
227 mechanically broken with a magnalyser at 6500rpm for 30 seconds (4 times),
228 and genomic DNA was sonicated for 20 cycles of 30 seconds ON/OFF in
229 presence of 0.5% SDS added before the sonication step. Samples were
230 centrifuged at 13000rpm for 15 min at 4°C, and chromatin (supernatant
231 phase) was quantified by Bradford. For each IP, 1/10 of the total extract was
232 kept as INPUT for final normalization. Chromatin extracts (500µg) were
233 incubated at 4°C o/n with a specific antibody. In parallel, magnetic beads
234 (Dynabeads® Magnetic, Thermo Fisher Scientific) were incubated with BSA 5
235 mg/ml at 4°C o/n. The magnetic beads were washed twice with FA lysis buffer
236 and resuspended with the same volume of FA lysis buffer containing a
237 protease inhibitor cocktail (beads 50% v/v). The chromatin extracts with a
238 specific antibody were incubated with 30µl of magnetic beads for 4h at 4°C on
239 a rotating wheel. The magnetic beads were then washed twice with FA lysis
240 buffer, twice with FA 500 (50mM HEPES KOH pH 7.5, 500mM NaCl, 1mM
241 EDTA pH 8, 1%Triton X-100, 0.1% sodium deoxycholate), once with Buffer III
242 (20mM Tris-HCl pH 8, 1mM EDTA pH 8, 250mM LiCl, 0.5% NP40, 0.5%

243 sodium deoxycholate) and once with TE 1X (100mM Tris-HCl pH 8, 10mM
244 EDTA pH 8). DNA was eluted with 200µl of elution buffer (50mM Tris-HCl pH
245 7.5, 1% SDS) at 65°C for 20 minutes. IP and INPUT DNAs were finally de-
246 crosslinked with proteinase K (Roche) (0.4 µg/µl) for 2 hours at 42°C, and o/n
247 at 65°C. The decrosslinked IP and INPUT DNAs were purified (Promega,
248 Wizard® Genomic DNA Purification Kit). IP and INPUT (2µl) were quantified
249 by qPCR with SYBR® Green PCR Master Mix (Applied Biosystems) using
250 specific primers.
251 The following antibodies were used: a rabbit polyclonal αHA antibody (Enzo),
252 a rabbit polyclonal αYra1 antibody and corresponding pre-immune (Stutz
253 laboratory).

254 **Ubiquitination and Sumoylation assays**

255 Ubiquitination and sumoylation assays were performed essentially as
256 described (8, 29, 30) using cells transformed with a plasmid expressing His6-
257 Ubi or His6-SUMO from a copper inducible promoter (P_{CUP1}). Briefly
258 Ubiquitin/SUMO expression was induced with 0.1 mM $CuSO_4$ overnight or for
259 3h. Cell cultures (200 ml) at OD_{600}=1 were collected adding TCA 5% for 20
260 minutes to allow protein precipitation. Cell pellets were washed twice with
261 acetone 100%. Dry pellets were resuspended with 1ml of Guanidinium buffer
262 (100 mM sodium phosphate at pH 8, 10 mM Tris-HCl, 6 M guanidinium, 10
263 mM imidazole, 0.2% Triton X-100, 10 mM NEM, complete protease inhibitor
264 mix [Roche]) prior to cell disruption with glass beads in a magnalyser (6
265 cycles at 6500 rpm for 1 minute).
266 Cells lysates were spun at 13000 rpm for 20 min. Between 5-8 mg of protein
267 from the supernatant was incubated with 100µl of Ni-NTA acid-agarose

268 (Qiagen) for 2h at room temperature on a rotating wheel. Agarose beads were
269 washed once with Guanidinium buffer and three times with Urea buffer (100
270 mM sodium phosphate at pH 6.8, 10 mM Tris-HCl, 8M urea, 20 mM
271 imidazole, 0.2% Triton X-100, complete protease inhibitor mix [Roche]). His6-
272 ubiquitinated and His6-SUMOylated proteins were eluted with 40 µl of Sample
273 Buffer and boiled for 5 min at 95°C. 20µl samples were analyzed by Western
274 blot with the relevant antibodies: αHIS for ubiquitinated or SUMOylated
275 proteins, αHA for ubiquitinated or SUMOylated HA-Yra1. Input samples were
276 also precipitated with TCA 5%, the pellets resuspended with Sample Buffer
277 and boiled 5 min at 95°C to be analyzed by Western Blot with αHA for HA-
278 Yra1 and αPgk1 as loading control.

279 **FISH experiments**

280 The FISH experiments on the *YRA1* shuffled strains deleted for various
281 ubiquitin ligases were done essentially as described in (8), while the FISH
282 experiments on the different HA-YRA1 integrated strains were performed as
283 described in (31). In the latter case, images were taken with the Zeiss
284 LSM700 confocal microscope using laserline 405 nm for DAPI detection and
285 laserline 555 nm for Cy3. Transmission light images were taken to see the cell
286 shape. In both cases Poly(A)$^+$mRNA in situ hybridization was performed with
287 a Cy3-labeled oligo-dT$_{(50)}$ probe.

288 **Colony Forming Unit Assay (CFU)**

289 Three serial dilutions (200/100/50) of exponentially growing cells in
290 SCLGg medium were plated on SCLGg Gal 2% or SCLGg Gal 3%-Raf 1% or
291 SCLGg Glu 2% and incubated at 25°C for 5 days. CFUs were counted and the

292 % of colonies was expressed as CFU relative to the CFU grown on SCLGg Glu

293 2% (control).

294

295 **RESULTS**
296

297 **Yra1 is modified by the SUMO-targeted E3 ubiquitin ligase Slx5-Slx8**

298 Previous work from our laboratory showed that Yra1 ubiquitination by
299 Tom1 elicits Yra1 dissociation from mRNPs, presumably in the context of the
300 nuclear pore complex (NPC), allowing proper mRNP export into the cytoplasm
301 (8). Intriguingly, Yra1 ubiquitination is not fully abrogated in the *Δtom1* mutant,
302 suggesting that other E3 ligases are involved in Yra1 regulation, possibly for
303 other Yra1 functions. In view of the putative role of Yra1 in genome stability,
304 we wondered whether this protein could be modified by SUMO-dependent
305 ubiquitination. Consistently, we identified the SUMO-targeted E3 ubiquitin
306 ligase (STUbL) complex Slx5-Slx8 to be responsible for Yra1 ubiquitination
307 together with Tom1 (**Fig 1**).

308 **Fig 1: Yra1 is a sumoylated protein targeted for ubiquitination by the**
309 **SUMO-dependent ubiquitin ligase Slx5-8. (A)** Yra1 ubiquitination depends
310 on the STUbL Slx5-Slx8 and Tom1. Ubiquitination assay of shuffled *HA-YRA1*
311 in wild-type and in *Δtom1*, *Δslx8*, *Δslx5*, *Δslx8Δtom1*, *Δslx5Δtom1* and
312 *Δslx8Δslx5* mutant backgrounds. Strains were transformed with a copper
313 inducible His-Ubiquitin expressing 2μ plasmid (+) or an empty vector (-). His-
314 Ubiquitin was induced with copper over night. His-Ubiquitinated proteins were
315 affinity-purified and the Ubiquitinated forms of Yra1 detected by Western Blot
316 with αHA antibodies. Western Blot of input samples with αHA antibody was
317 used to assess input Yra1 levels. One representative experiment of 3 is
318 shown. **(B)** Yra1 is sumoylated. Sumoylation assay in wild-type and *HA-YRA1*
319 backgrounds. Strains were transformed with a copper inducible His-SUMO
320 expressing 2μ plasmid (+) or with an empty vector (-). His-SUMO was induced
321 with copper for 3h. His-sumoylated proteins were affinity-purified and the
322 sumoylated forms of Yra1 detected by Western Blot with αHA antibodies.
323 Western Blot of input samples with αHA was used to assess input Yra1 levels.
324 One representative experiment of 3 is shown. **(C)** Yra1 is sumoylated by
325 Siz1/Siz2. Yra1 sumoylation assay in wild-type as well as *Δsiz1, Δsiz1/siz2,*
326 *Δsiz2* and *mms21* mutant backgrounds. Strains were transformed with a
327 copper inducible His-SUMO expressing 2μ plasmid. His-SUMO was induced
328 with copper for 3h. His-SUMOylated proteins were affinity purified and the
329 SUMOylated forms of Yra1 detected by Western Blot with an αYrα1 antibody.
330 Western Blot of input samples with αYra1 was used to assess input Yra1
331 levels. One representative experiment of 2 is shown.

332 The ubiquitination assay of HA-Yra1 in wild-type and in *Δtom1*, *Δslx5,*
333 *Δslx8, Δslx5Δslx8, Δslx5Δtom1, Δslx8Δtom1* mutant backgrounds showed that
334 the Yra1 ubiquitination detected in the *Δtom1* mutant was completely
335 abrogated in the *Δslx5Δtom1* and *Δslx8Δtom1* double mutants (**Fig 1A**),
336 indicating a role for both the Slx5-Slx8 and Tom1 E3 ligases in Yra1
337 regulation. Since the Slx5-Slx8 E3 ligase complex is stimulated by substrate
338 sumoylation (32), and in view of the reported identification of Yra1 as
339 potentially sumoylated in a proteome-wide study (33), we confirmed that Yra1
340 is indeed sumoylated (**Fig 1B** and **1C**). Both Siz1 and Siz2 SUMO E3 ligases
341 are involved in this modification as Yra1 sumoylation is fully abrogated in the
342 *Δsiz1Δsiz2* double mutant background (**Fig 1C**). Furthermore, Yra1 is de-
343 sumoylated by the SUMO protease Ulp1 as Yra1 sumoylation increased in the
344 *ulp1* temperature-sensitive (*ts*) mutant (**Supplementary Fig S1A).** These data
345 support the hypothesis that Yra1 is regulated both by sumoylation and
346 ubiquitination. In addition, HA-Yra1 ubiquitination was increased in the *ulp1 ts*
347 mutant compared to a wild-type background, suggesting a possible
348 stimulating effect of sumoylation on ubiquitination (**Supplementary Fig S1B)**.
349 Known targets of Slx5-Slx8 are controlled by ubiquitin-dependent
350 proteasomal degradation (34-38). To define whether Yra1 ubiquitination by
351 Slx5-Slx8 may target Yra1 to degradation, we used metabolic depletion to
352 examine Yra1 turnover. Because *YRA1* is essential, an HA-tagged version of
353 *YRA1* was expressed from a galactose-inducible promoter on a plasmid
354 transformed into a strain expressing a wild-type *YRA1* gene. Switching cells
355 from galactose to glucose-containing medium represses *GAL-HA-YRA1* gene
356 expression and allows following the decay of the HA-Yra1 protein in different

357 genetic backgrounds. Under metabolic glucose repression, HA-Yra1 has a
358 half-life of 3.8h **(Supplementary Fig S2A)**. No significant stabilization of HA-
359 Yra1 protein was detected in *Δslx8, Δslx5, Δtom1* or *Δslx8Δtom1*
360 **(Supplementary Fig S2B and S2C)**, suggesting that ubiquitination by Slx5-
361 Slx8 does not lead to Yra1 degradation by the proteasome.

362 We previously proposed that Yra1 regulation by Tom1 is linked to the
363 function of Yra1 in mRNP export (1, 8). Visualization of poly(A)+ RNA
364 distribution by fluorescence in situ hybridization (FISH) in the *Δslx5* and *Δslx8*
365 single mutants did not show any nuclear poly(A)+ RNA retention while the
366 *Δslx5Δtom1* (32.3%) and *Δslx8Δtom1* (26%) double mutants had mRNA
367 export defects comparable to the *Δtom1* mutant (30.8%) (**Supplementary Fig**
368 **S3A**). These observations suggest that Yra1 ubiquitination by Slx5-Slx8 may
369 regulate a function of Yra1 distinct from mRNA export.

370

371 **Loss of the Yra1 C-box sensitizes the genome to DSBs**

372 Since our data indicate that Yra1 is modified by Slx5-Slx8, a STUbL
373 important for genome stability (39), we examined whether the abrogation of
374 Yra1 ubiquitination induces defects in genome integrity. For this purpose, we
375 used the *HA-yra1allKR* mutant that cannot be ubiquitinated since all the
376 Lysines (K) are replaced by Arginines (R) **(Fig 2A)** (8).

377 **Fig 2: The Yra1 C-box, but not Yra1 ubiquitination, is important for**
378 **genome stability. (A)** Scheme of Yra1 mutants used in this study. **(B)** Left:
379 Western Blot analysis of HA-Yra1 levels in integrated *HA-YRA1 WT*, *HA-*
380 *yra1(1-210), HA-yra1allKR,* was performed using an αHA antibody; an αPgk1
381 antibody was used as loading control. One representative Western blot is
382 shown. Right: Western blot quantification showing the HA-Yra1/Pgk1 ratio of
383 three experiments with relative standard error of the mean. The
384 quantifications were performed using Lycor Software. **(C)** Spot test analysis of
385 confluent cells at 25°C, 30°C, 34°C, 37°C of *YRA1 WT* (No Tag), integrated
386 *HA-YRA1 WT*, *HA-yra1(1-210)*, and *HA-yra1allKR* strains on YEPD 2%
387 Glucose. **(D)** Spot test analysis on YEPD 2% Glu, Zeocin 25 µg/ml, 50 µg/ml
388 and 100 µg/ml at 25°C of confluent cells of integrated *HA-YRA1 WT* and *HA-*
389 *yra1* mutants as well as *Δrad52* strains.
390
391 We also used the *HA-yra1(1-210)* mutant which codes for a protein that
392 is still ubiquitinated (data not shown) but lacks the highly conserved 16 C-
393 terminal amino-acids **(Fig 2A)**. Because Yra1 levels are maintained through
394 splicing autoregulation, the intron was retained in both wild-type and mutant
395 HA-YRA1 constructs to limit the potential toxic effect of Yra1 overexpression (4,
396 10, 12, 13, 16). Although the C-terminal domain has been implicated in splicing
397 inhibition (4), the HA-yra1(1-210) protein is only mildly overexpressed
398 compared to wild-type HA-Yra1 or the HA-yra1allKR mutant protein and
399 presents only a slight growth defect at 25°C (**Fig 2B and C**). Both mutants are
400 thermosensitive as shown by spot test analysis at different temperatures (25°C-
401 30°C-34°C-37°C) (**Fig 2C**). FISH analysis did not reveal any nuclear poly(A)+
402 RNA retention at 25°C indicating that the two mutants have no mRNA export

403 defect in the conditions used in this study (**Supplementary Fig S3B**) (7).
404 Interestingly, additional spot test analyses in the presence of Zeocin, indicated
405 that the *HA-yra1(1-210)* but not the *HA-yra1allKR* mutant is sensitive to this
406 genotoxic drug (**Fig 2D**). This observations indicates that the Yra1 C-box is
407 important for genome stability in the presence of DNA double strand breaks
408 (DSBs) while Yra1 ubiquitination is not.
409

410 **Yra1 is recruited to an irreparable DSB (HO cut)**

411 To obtain more direct evidence for a possible role of Yra1 in the DNA
412 damage response pathway (DDR), we induced an irreparable DSB at the
413 MAT locus using a galactose-inducible HO endonuclease as described (25)
414 (**Supplementary Fig S4A**). Consistent with the irreparable nature of the
415 induced HO cuts, these strains do not grow on galactose (**Supplementary**
416 **Fig S5A**). Importantly, Yra1 recruitment at the HO cut, examined by ChIP with
417 an αYra1 antibody, was significant at regions close to the DSB after 2h of HO
418 induction (**Fig 3A**).

419 **Fig 3: Yra1 is recruited to an irreparable DSB HO cut site. (A)** Yra1
420 recruitment at the HO cut site was defined by ChIP with an αYra1 antibody
421 after 0.5h, 1h, 2h and 4h of HO endonuclease induction with galactose using
422 the GA6844 strain described in (25). The 2h Glucose time point was used as
423 no cut control. ChIP values are indicated as percentage of input at 0.6Kb,
424 1.6Kb, 4.5Kb, 9.6Kb and 23Kb from the HO cut. The average of 6
425 experiments is shown with corresponding standard error of the mean. Two
426 way ANOVA test was performed with multiple comparisons; P values < 0.05
427 (*), < 0.01 (**), < 0.001 (***) that refer to Glu 2h (no cut) are shown. **(B)** Yra1
428 mutants are differentially recruited to the irreparable HO cut site. ChIP using
429 αHA antibody of HA-Yra1 WT, HA-yra1(1-210), HA-yra1allKR, Yra1WT (no
430 tag) at 0.6 Kb from the HO cut site after 2h of HO induction with Galactose
431 using the strains with *HA-YRA1 WT* or mutants integrated in strain GA6844
432 described in (25). The 2h Glucose time point was taken as no cut control.
433 ChIP values are shown as percentage of input. The average of 3 independent
434 experiments is shown with corresponding standard error of the mean. **(C)**
435 RPA recruitment to the HO cut site in *HA-YRA1 WT* and *HA-yra1* mutants.
436 ChIP using αRPA antibody at 0.6 Kb from the HO cut site after 2h of HO
437 induction with Galactose in the same strains as in (B). The 2h Glucose time
438 point was taken as no cut control. ChIP values are indicated as percentage of
439 input. The average of 3 independent experiments is shown with
440 corresponding standard error of the mean.

441

442 Considering that the efficiency of the cut is nearly 100% after 30' of HO
443 induction (25) (**Supplementary Fig S6A**), the recruitment after 2h suggests it
444 may depend on extensive resection.

445 To define whether the sensitivity to Zeocin of the *HA-yra1(1-210)*
446 mutant may be due to its impaired recruitment to DSB loci, sequences
447 encoding HA-tagged wild-type or mutant Yra1 (*HA-YRA1 WT*, *HA-yra1(1-210)*
448 and *HA-yra1allKR*) were integrated into the irreparable HO DSB strain at the
449 *YRA1* locus and the recruitment of these different HA-Yra1 proteins at the HO
450 cut was examined by ChIP using αHA antibodies after 2h in galactose (**Fig**
451 **3B**), which induces efficient HO cleavage in both wild-type and mutant strains
452 (**Supplementary Fig S6B)**. These experiments show that the HA-yra1allKR
453 protein is recruited to the HO cut site to similar levels as the HA-Yra1 WT in
454 Galactose (HO cut) (**Fig 3B**). In contrast, although in this experiment the HA-
455 yra1(1-210) protein is expressed to slightly higher levels than HA-Yra1 WT
456 (**Supplementary Fig S5B and S5C)**, its binding to the HO site does not
457 increase in galactose, suggesting that the Yra1 C-terminal region is important
458 for Yra1 recruitment to the DSB. Since Yra1 is recruited to the HO cut 2h after
459 Gal induction, once there has been extensive resection, we asked whether
460 RPA binding to the HO cut might vary in the different *HA-yra1* mutants. RPA
461 association was not affected in the *HA-yra1* mutants despite the lack of HA-
462 yra1(1-210) recruitment (**Fig 3C**), suggesting that RPA binding is probably not
463 dependent on Yra1 recruitment.
464

465 **The Yra1 C-terminal region is important for DSB repair (HO cut)**

466 Since irreparable DSBs relocate to the nuclear pore in G1/S phase (26)
467 within 2h after cut induction (25), one possibility is that Yra1 recruitment to
468 irreparable DSB is the consequence of HO cut re-localization to pores. To
469 exclude this possibility, we took advantage of an HO cut reparable system

470 (**Supplementary Fig S4B**) (28), since the DSB repair occurs within the
471 nuclear interior (40, 41). To define whether the *HA-yra1* mutants may be
472 defective in DSB repair, the *HA-YRA1 WT*, *HA-yra1(1-210)* and *HA-*
473 *yra1ΔallKR* sequences were integrated at the *YRA1* locus of the reparable HO
474 DSB strain and the percentage of cells surviving under HO cut induction was
475 examined.

476 Three serial dilutions of exponentially growing cells were plated on
477 galactose 2% or galactose 3%-raffinose 1% to induce the HO cut, and on
478 glucose 2% to repress HO endonuclease expression. CFUs were counted as
479 an indication of cells able to repair the DSB in the *HA-YRA1 WT*, *HA-yra1(1-*
480 *210)*, *HA-yra1allKR* strains transformed with a pGAL-HO endonuclease
481 plasmid or Empty Vector; a *No-Tag* and a *Δrad52* strain transformed with the
482 Empty Vector only were used as controls as these two strains contain an
483 endogenous pGAL-HO endonuclease sequence (**Fig 4A**).

484 **Fig 4: Survival under persistant induction of a reparable HO cut. (A)** The
485 Yra1 C-box is important for DSB repair. Three serial dilutions (200/100/50) of
486 exponentially growing cells of NA17 strain (28) containing integrated *HA-*
487 *YRA1 WT* (WT), *HA-yra1(1-210)*, *HA-yra1allKR* and transformed with pGAL-
488 HO endonuclease containing plasmid or Empty Vector, as well as of No-Tag
489 (NA17) and *Δrad52* strains containing endogenous pGAL-HO endonuclease
490 and transformed with an Empty Vector were prepared. Diluted cells were
491 plated on SCLGg Gal 2% or Gal 3%-Raf1% to constantly induce HO cut, and
492 on SCLGg Glu 2% to repress HO endonuclease expression. The percentage
493 of colonies was determined as the relative number of Colony Forming Units
494 (CFUs) in each strain plated on SCLGg Gal 2% or Gal 3%-Raf1% compared
495 to the one plated on SCLGg Glu 2%. To normalize the variability in growth
496 due to the different media condition, the CFUs of each strain transformed with
497 pGAL-HO endonuclease were normalized to the corresponding strain
498 transformed with the empty vector (%CFU= (%CFU on SCLGg Gal 2% pGAL-
499 HO/EV)/ (% CFU on SCLGg Glu 2% pGAL-HO/EV). The average of 3
500 independent experiments for each condition SCLGg Gal 2%/ Glu 2% and
501 SCLGg Gal 3%-Raf 1%/ Glu 2% is shown with corresponding standard error
502 of the mean. One way ANOVA test was performed with multiple comparisons
503 and P value < 0.001 (**) is shown on the graph referring to *HA-YRA1 WT*. **(B)**
504 Yra1 C-box is important for DSB repair. Spot test analysis on Leu- SCLGg Glu
505 2%, SCLGg Gal 2%, SCLGg Gal 3%-Raf 1%, at 25°C of exponentially
506 growing *HA-YRA1 WT* (WT), *HA-yra1(1-210)*, *HA-yra1allKR* (transformed with
507 pGAL-HO endonuclease containing plasmid or Empty Vector); No-Tag and
508 *Δrad52* strains (containing endogenous pGAL-HO endonuclease sequence

509 and transformed with an empty vector) served as controls. One representative
510 experiment out of 3 is shown.
511
512 Interestingly, like the *Δrad52* control strain, the *HA-yra1(1-210)* mutant
513 was not able to grow on galactose when the reparable HO cut is induced,
514 indicating that the Yra1 C-box is important for DSB repair. This effect was
515 confirmed by spot test analysis (**Fig 4B**). Moreover, although both *HA-yra1*
516 mutants have comparable cut efficiency after 2h in Galactose
517 (**Supplementary Fig S6C),** the *HA-yra1ΔallKR* showed no growth defect
518 under HO cut induction whether in the CFU assay or the spot test, indicating
519 that Yra1 ubiquitination is not required for DSB repair (**Fig 4A and 4B**).
520 Overall these observations support the view that Yra1 is important for
521 DSB repair in a process dependent on the 16 amino acids C-terminal region.
522 Absence of this domain may result in the inability to repair HO cuts possibly
523 because of the reduced capacity of Yra1 to interact with the DSB.

525 **DISCUSSION**
526

527 This study strengthens the importance of Yra1 in genome stability. In
528 particular, our data provide evidence that the Yra1 C-terminal box is crucial for
529 DSB repair. We have started to investigate the sensitivity of *yra1* mutants to
530 DNA damage based on the observation that Yra1 is not only sumoylated by
531 Siz1-Siz2 but also ubiquitinated by Slx5-Slx8, a SUMO-dependent E3 ligase
532 important for genome stability (**Fig 1**). However, our data indicate that Yra1
533 ubiquitination is not important for DSB repair since the *HA-yra1allKR* mutant
534 that completely abrogates Yra1 ubiquitination (8) does not display any genetic
535 instability phenotypes.

536 To investigate the effect of Yra1 on genome stability, we rather took
537 advantage of the *HA-yra1(1-210)* mutant that lacks the Yra1 C-box domain
538 (**Fig 2**) without any obvious mRNA export defect (**Supplementary Fig S3**).
539 Interestingly, our data show that the *HA-yra1(1-210)* mutant is sensitive to the
540 DSB inducing genotoxic agent Zeocin (**Fig 2**). In line with these results, it was
541 recently published that the DAmP allele of *YRA1* is specifically sensitive to
542 Zeocin (18). Overall, these observations suggest that lack of the Yra1 C-box
543 or reduced levels of Yra1 either promote DSBs or impair DSB repair.

544 A recent study has revealed that Npl3, an RNA binding protein involved
545 in mRNP biogenesis, contributes to DSB resection by ensuring efficient
546 production of *EXO1* mRNA (42). While Npl3 was proposed to have an
547 indirect role in repair, our observations indicate that Yra1 is recruited to an
548 irreparable DSB after 2h of cut induction and therefore extensive resection,
549 consistent with a direct role of Yra1 in DSB repair (**Fig 3B**). Importantly, the

550 recruitment to an irreparable DSB does not depend on Yra1 ubiquitination but
551 requires the conserved C-box suggesting this domain may be involved in
552 repair, although it has no effect on RPA binding to the locus (**Fig 3B and 3C**).
553 However, we cannot fully exclude that Yra1 recruitment to irreparable DSBs
554 may be the consequence of HO cut re-localization to the nuclear pore that
555 occurs within 2h after cut induction (25). Furthermore, we also examined
556 whether the irreparable DSB can be repaired by alternative pathways such us
557 Non Homologous End Joining (NHEJ) (19) or Break Induced Repair (BIR)
558 (26) by inducing the HO cut in the *HA-yra1* mutants for 2h and plating the
559 cells on Glucose. The *HA-yra1allKR* and *HA-yra1(1-210)* mutants showed
560 survival rates comparable to *HA-YRA1 WT* indicating that the Yra1 C-box and
561 Yra1 ubiquitination do not contribute to alternative repair pathways (data not
562 shown).

563 To directly address DSB repair efficiency in the *HA-yra1allKR* and *HA-*
564 *yra1(1-210)* mutants, we used the HO reparable system described in (28).
565 Unfortunately, we were unable to observe significant recruitment of Yra1 to
566 this type of DSB by ChIP, probably because the HO reparable system is more
567 dynamic (data not shown). However, an independent recent study identified
568 Yra1 at an HO-induced reparable DSB using ChAP-MS (Chromatin Affinity
569 Purification with mass spectrometry) (18). These data indicate that Yra1 is
570 recruited to the DSB locus also when the HO cut is located within the nucleus
571 (40, 43). Thus, the observed Yra1 binding at the irreparable HO cut (**Fig 3A**
572 **and 3B**) may be specific rather than the indirect consequence of DSB
573 relocalization to the nuclear periphery.

574 Besides detecting Yra1 at reparable DSBs, the recent study by Wang
575 et al. (18) also shows that a Yra1 DAmP hypomorph mutant has a defect in
576 global DSB repair following Zeocin treatment comparable to that observed in
577 the absence of the central Rad52 repair protein. As discussed by the authors,
578 this global effect probably results from the reduced expression of Rad51 due
579 to defective mRNA biogenesis and export activity in the presence of low levels
580 of Yra1. The same study investigated the importance of Yra1 in the repair of a
581 single HO cut using the Yra1 anchor away system. These experiments were
582 unable to demonstrate a role for Yra1 in this process possibly because the
583 conditions used to deplete Yra1 by anchor away were not optimal.

584 Since irreparable DSBs lead to cell death (19), we addressed the
585 critical role of Yra1 in DSB repair by defining the repair efficiency of the *HA-*
586 *yra1allKR* and □□□*yra1(1-210)* mutants based on survival under induction of
587 a reparable HO cut (**Fig 4**). Interestingly, while the *HA-yra1allKR* mutant has
588 not effect, the *HA-yra1(1-210)* mutant exhibits very poor survival, comparable
589 to that observed in *Δrad52* (**Fig 4**). Since the *HA-yra1(1-210)* strain has no
590 obvious mRNA export phenotype and exhibits normal Rad51 levels
591 (**Supplementary Fig S3** and **S7**), the data support the hypothesis that Yra1
592 may play a direct role in DSB repair and that the C-box is required for its
593 recruitment to the damaged site (**Fig 3B**). In conclusion, one view is that C-
594 box-dependent Yra1 recruitment is important for repair possibly by favoring
595 optimal Rad52 action and homologous recombination at the DSB.

596 While our data show that Yra1 ubiquitination is not required for DSB
597 repair, we cannot exclude that Yra1 sumoylation and ubiquitination by Slx5-
598 Slx8 may facilitate relocalization of irreparable DSBs to nuclear pores (25,

599 26). The physiological relevance of irreparable DSB relocation to the nuclear
600 periphery is still not fully clear. It has been speculated that it leads to
601 proteasomal degradation of DSB-bound proteins targeted by the STUbL Slx5-
602 Slx8 (25) to induce alternative repair pathways such us Break Induced
603 Replication (26). In that respect, our data show that ubiquitination by Slx5-
604 Slx8 does not lead to Yra1 degradation (**Supplementary Fig S2**).
605 Furthermore, Yra1 ubiquitination is not required for survival after irreparable
606 DSB induction suggesting that it is not important for non-canonical repair
607 (data not shown).

608 In summary, this work indicates that at physiological expression levels,
609 Yra1 is beneficial for genome stability by facilitating the repair of DSBs in a C-
610 box-dependent and sumoylation/ubiquitination independent manner. Future
611 studies should address how Yra1 recruitment to DSBs may contribute to
612 repair through homologous recombination.

613 **ACKNOWLEDGMENTS**

614 We would like to thank D. Picard and T. Halazonetis as well as members of
615 the lab for discussions; we also are grateful to S. Gasser and M. Kupiec for
616 strains and plasmids.

617 **AUTHOR CONTRIBUTIONS**

618 V.I., E.T., and BP designed and performed experiments. N.Y.M, A.Z, V.G.M
619 and G.S. performed experiments. V.I. and F.S. conceived experiments and
620 wrote the paper.

621

622

623 **REFERENCES**

624 1. Tutucci E, Stutz F. Keeping mRNPs in check during assembly and
625 nuclear export. Nat Rev Mol Cell Biol. 2011;12(6):377-84.
626 2. Portman DS, O'Connor JP, Dreyfuss G. YRA1, an essential
627 Saccharomyces cerevisiae gene, encodes a novel nuclear protein with
628 RNA annealing activity. RNA. 1997;3(5):527-37.
629 3. Stutz F, Bachi A, Doerks T, Braun IC, Seraphin B, Wilm M, et al. REF,
630 an evolutionary conserved family of hnRNP-like proteins, interacts with
631 TAP/Mex67p and participates in mRNA nuclear export. RNA.
632 2000;6(4):638-50.
633 4. Preker PJ, Guthrie C. Autoregulation of the mRNA export factor Yra1p
634 requires inefficient splicing of its pre-mRNA. RNA. 2006;12(6):994-1006.
635 5. Strasser K, Masuda S, Mason P, Pfannstiel J, Oppizzi M, Rodriguez-
636 Navarro S, et al. TREX is a conserved complex coupling transcription
637 with messenger RNA export. Nature. 2002;417(6886):304-8.
638 6. Burd CG, Dreyfuss G. Conserved structures and diversity of functions of
639 RNA-binding proteins. Science. 1994;265(5172):615-21.
640 7. Zenklusen D, Vinciguerra P, Strahm Y, Stutz F. The yeast hnRNP-Like
641 proteins Yra1p and Yra2p participate in mRNA export through interaction
642 with Mex67p. Mol Cell Biol. 2001;21(13):4219-32.
643 8. Iglesias N, Tutucci E, Gwizdek C, Vinciguerra P, Von Dach E, Corbett
644 AH, et al. Ubiquitin-mediated mRNP dynamics and surveillance prior to
645 budding yeast mRNA export. Genes Dev. 2010;24(17):1927-38.
646 9. Dong S, Li C, Zenklusen D, Singer RH, Jacobson A, He F. YRA1
647 autoregulation requires nuclear export and cytoplasmic Edc3p-mediated
648 degradation of its pre-mRNA. Molecular cell. 2007;25(4):559-73.
649 10. Espinet C, de la Torre MA, Aldea M, Herrero E. An efficient method to
650 isolate yeast genes causing overexpression-mediated growth arrest.
651 Yeast. 1995;11(1):25-32.
652 11. Reed R, Hurt E. A conserved mRNA export machinery coupled to pre-
653 mRNA splicing. Cell. 2002;108(4):523-31.
654 12. Preker PJ, Kim KS, Guthrie C. Expression of the essential mRNA export
655 factor Yra1p is autoregulated by a splicing-dependent mechanism. RNA.
656 2002;8(8):969-80.
657 13. Rodriguez-Navarro S, Strasser K, Hurt E. An intron in the YRA1 gene is
658 required to control Yra1 protein expression and mRNA export in yeast.
659 EMBO Rep. 2002;3(5):438-42.
660 14. Fong CM, Arumugam A, Koepp DM. The Saccharomyces cerevisiae F-
661 box protein Dia2 is a mediator of S-phase checkpoint recovery from DNA
662 damage. Genetics. 2013;193(2):483-99.
663 15. Swaminathan S, Kile AC, MacDonald EM, Koepp DM. Yra1 is required
664 for S phase entry and affects Dia2 binding to replication origins. Mol Cell
665 Biol. 2007;27(13):4674-84.
666 16. Gavalda S, Santos-Pereira JM, Garcia-Rubio ML, Luna R, Aguilera A.
667 Excess of Yra1 RNA-Binding Factor Causes Transcription-Dependent
668 Genome Instability, Replication Impairment and Telomere Shortening.
669 PLoS Genet. 2016;12(4):e1005966.
670 17. Garcia-Rubio M, Aguilera P, Lafuente-Barquero J, Ruiz JF, Simon MN,
671 Geli V, et al. Yra1-bound RNA-DNA hybrids cause orientation-

672 independent transcription-replication collisions and telomere instability.
673 Genes Dev. 2018;32(13-14):965-77.
674 18. Wang P, Byrum S, Fowler FC, Pal S, Tackett AJ, Tyler JK. Proteomic
675 identification of histone post-translational modifications and proteins
676 enriched at a DNA double-strand break. Nucleic Acids Res.
677 2017;45(19):10923-40.
678 19. Zhao X, Wei C, Li J, Xing P, Li J, Zheng S, et al. Cell cycle-dependent
679 control of homologous recombination. Acta Biochim Biophys Sin
680 (Shanghai). 2017;49(8):655-68.
681 20. Symington LS, Gautier J. Double-strand break end resection and repair
682 pathway choice. Annu Rev Genet. 2011;45:247-71.
683 21. Altmannova V, Kolesar P, Krejci L. SUMO Wrestles with Recombination.
684 Biomolecules. 2012;2(3):350-75.
685 22. Jalal D, Chalissery J, Hassan AH. Genome maintenance in
686 Saccharomyces cerevisiae: the role of SUMO and SUMO-targeted
687 ubiquitin ligases. Nucleic Acids Res. 2017;45(5):2242-61.
688 23. Ulrich HD. Ubiquitin and SUMO in DNA repair at a glance. J Cell Sci.
689 2012;125(Pt 2):249-54.
690 24. Sarangi P, Zhao X. SUMO-mediated regulation of DNA damage repair
691 and responses. Trends Biochem Sci. 2015;40(4):233-42.
692 25. Nagai S, Dubrana K, Tsai-Pflugfelder M, Davidson MB, Roberts TM,
693 Brown GW, et al. Functional targeting of DNA damage to a nuclear pore-
694 associated SUMO-dependent ubiquitin ligase. Science.
695 2008;322(5901):597-602.
696 26. Horigome C, Bustard DE, Marcomini I, Delgoshaie N, Tsai-Pflugfelder M,
697 Cobb JA, et al. PolySUMOylation by Siz2 and Mms21 triggers relocation
698 of DNA breaks to nuclear pores through the Slx5/Slx8 STUbL. Genes
699 Dev. 2016;30(8):931-45.
700 27. Horigome C, Oma Y, Konishi T, Schmid R, Marcomini I, Hauer MH, et al.
701 SWR1 and INO80 chromatin remodelers contribute to DNA double-
702 strand break perinuclear anchorage site choice. Mol Cell.
703 2014;55(4):626-39.
704 28. Agmon N, Liefshitz B, Zimmer C, Fabre E, Kupiec M. Effect of nuclear
705 architecture on the efficiency of double-strand break repair. Nat Cell Biol.
706 2013;15(6):694-9.
707 29. Bretes H, Rouviere JO, Leger T, Oeffinger M, Devaux F, Doye V, et al.
708 Sumoylation of the THO complex regulates the biogenesis of a subset of
709 mRNPs. Nucleic Acids Res. 2014;42(8):5043-58.
710 30. Bonnet A, Bretes H, Palancade B. Nuclear pore components affect
711 distinct stages of intron-containing gene expression. Nucleic Acids Res.
712 2015;43(8):4249-61.
713 31. Rahman S, Zenklusen D. Single-molecule resolution fluorescent in situ
714 hybridization (smFISH) in the yeast S. cerevisiae. Methods Mol Biol.
715 2013;1042:33-46.
716 32. Xie Y, Kerscher O, Kroetz MB, McConchie HF, Sung P, Hochstrasser M.
717 The yeast Hex3.Slx8 heterodimer is a ubiquitin ligase stimulated by
718 substrate sumoylation. J Biol Chem. 2007;282(47):34176-84.
719 33. Wohlschlegel JA, Johnson ES, Reed SI, Yates JR, 3rd. Global analysis
720 of protein sumoylation in Saccharomyces cerevisiae. J Biol Chem.
721 2004;279(44):45662-8.

722 34. Nixon CE, Wilcox AJ, Laney JD. Degradation of the Saccharomyces
723 cerevisiae mating-type regulator alpha1: genetic dissection of cis-
724 determinants and trans-acting pathways. Genetics. 2010;185(2):497-
725 511.
726 35. Schweiggert J, Stevermann L, Panigada D, Kammerer D, Liakopoulos D.
727 Regulation of a Spindle Positioning Factor at Kinetochores by SUMO-
728 Targeted Ubiquitin Ligases. Dev Cell. 2016;36(4):415-27.
729 36. Su XA, Dion V, Gasser SM, Freudenreich CH. Regulation of
730 recombination at yeast nuclear pores controls repair and triplet repeat
731 stability. Genes Dev. 2015;29(10):1006-17.
732 37. Westerbeck JW, Pasupala N, Guillotte M, Szymanski E, Matson BC,
733 Esteban C, et al. A SUMO-targeted ubiquitin ligase is involved in the
734 degradation of the nuclear pool of the SUMO E3 ligase Siz1. Mol Biol
735 Cell. 2014;25(1):1-16.
736 38. Xie Y, Rubenstein EM, Matt T, Hochstrasser M. SUMO-independent in
737 vivo activity of a SUMO-targeted ubiquitin ligase toward a short-lived
738 transcription factor. Genes Dev. 2010;24(9):893-903.
739 39. Zhang C, Roberts TM, Yang J, Desai R, Brown GW. Suppression of
740 genomic instability by SLX5 and SLX8 in Saccharomyces cerevisiae.
741 DNA Repair (Amst). 2006;5(3):336-46.
742 40. Bystricky K, Van Attikum H, Montiel MD, Dion V, Gehlen L, Gasser SM.
743 Regulation of nuclear positioning and dynamics of the silent mating type
744 loci by the yeast Ku70/Ku80 complex. Mol Cell Biol. 2009;29(3):835-48.
745 41. Mine-Hattab J, Rothstein R. Increased chromosome mobility facilitates
746 homology search during recombination. Nat Cell Biol. 2012;14(5):510-7.
747 42. Colombo CV, Trovesi C, Menin L, Longhese MP, Clerici M. The RNA
748 binding protein Npl3 promotes resection of DNA double-strand breaks by
749 regulating the levels of Exo1. Nucleic Acids Res. 2017;45(11):6530-45.
750 43. Dion V, Gasser SM. Chromatin movement in the maintenance of
751 genome stability. Cell. 2013;152(6):1355-64.
752
753

754

755 **SUPPLEMENTAL FIGURES**

756

757 **S1 Fig: Yra1 sumoylation promotes its ubiquitination.**

758 **(A)** Yra1 is de-SUMOylated by Ulp1. Sumoylation assay in wild-type and *ulp1*

759 temperature-sensitive (ts) mutant as described in Fig 1. One representative

760 experiment of 3 experiments is shown.

761 **(B)** Yra1 ubiquitination increases in the *ulp1 ts* mutant. Ubiquitination assay in

762 wild-type and *ulp1* temperature-sensitive mutant as described in Fig 1. One

763 representative experiment of 3 experiments is shown.

764 **S2 Fig: Ubiquitination by Slx5-Slx8 does not affect Yra1 half-life. (A)** Yra1
765 half-life is 3.8 h when using a metabolic Gal depletion assay. Protein stability
766 assay using metabolic depletion of *GAL-HA-YRA1* in the presence of the
767 endogenous wild-type *YRA1* gene. *YRA1* WT shuffle cells expressing HA-
768 Yra1 from the GAL promoter on a centromeric plasmid were grown over-night
769 in selective medium containing 2% galactose. Cells at OD=0.3 were shifted to
770 selective medium containing 2% glucose to repress *GAL-HA-YRA1* and
771 collected at time 0, 1h, 2h, 3h, 4h, 5h, 6h, and 7h following glucose addition.
772 HA-Yra1 protein levels were quantified by Western blot with an αHA antibody
773 and normalized to Pgk1 with αPgk1 as loading control, using fluorescent
774 secondary antibodies detected with the Lycor machine and analyzed with
775 LITE software. The average of 2 independent experiments is shown. **(B)**, **(C)**
776 Yra1 stability does not change in the absence of E3 ligases. Protein stability
777 assay using metabolic depletion of *GAL-HA-YRA1* in the *YRA1* WT shuffle
778 background combined with *Δslx5*, *Δslx8*, *Δtom1* and *Δslx8Δtom1*. Western
779 Blot analysis (B) and relative quantification (C) were performed as described
780 in (A). The average of 3 independent experiments (N3) is shown for the *Δslx5*,
781 *Δslx8*, *Δtom1* and *Δslx8Δtom*1 strains. Two way ANOVA statistical test with
782 multiple comparisons did not show any statistically significant difference (n.s)
783 between different yeast strains in the same time points.

784 **S3 Fig: The *Δslx5* , *Δslx8* and *yra1* mutants show no mRNA export defect**
785 **by FISH analysis. (A)** Fluorescent in situ hybridization (FISH) analysis of
786 poly(A)+ RNA localization using oligo(dT) probes in shuffled *HA-YRA1 WT* in
787 WT, *Δtom1*, *Δslx8*, *Δslx5*, *Δslx8Δtom1*, *Δslx5Δtom1* background and *mex67-5*
788 cells as control for mRNA export defect. The percent of cells showing poly(A)+
789 RNA accumulation in the nucleus is indicated in each panel. DAPI stains the
790 cell nucleus. **(B)** Fluorescent *in situ* hybridization (FISH) analysis of poly(A)+
791 RNA localization using oligo(dT) probes in integrated *HA-YRA1* WT, *HA-*
792 *yra1(1-210)*, *HA-yra1allKR* and *mex67-5* cells. Cells were grown exponentially
793 in YEPD 2% Glu at 25°C. *mex67-5* ts mutant was grown for an additional 1h
794 at 37°C. One representative image of nuclear staining (DAPI), oligo-dT Cy3
795 (poly(A)+ RNA), and Transmission Light with merged channels is shown for
796 each strain analyzed. The percent of cells showing poly(A)+ RNA
797 accumulation in the nucleus is shown in each panel.

798 **S4 Fig: Gal-induced HO-mediated irreparable and reparable DSB**
799 **systems. (A)** Scheme showing the Gal-induced HO-mediated irreparable
800 DSB described in (27). The HO endonuclease is expressed in the presence of
801 Galactose, inducing the HO cut at the Mat locus that cannot be repaired
802 because of the deletion of *HML* and *HMR*. **(B)** Scheme showing the Gal-
803 induced HO-mediated reparable DSB described in (28). The HO
804 endonuclease is expressed in the presence of Galactose, inducing the HO cut
805 at the KanMx cassette next to the URA3 locus. The repair of the DSB at the
806 HO cut is possible by HR thanks to the KanMX cassette at the LYS2 locus. If
807 this occurs, the repair will result in an HO insensitive KanMX cassette at the
808 URA3 locus as well as the loss of the short unique sequence surrounding the
809 initial HO cut site.
810

811 **S5 Fig: Growth phenotypes and protein levels in the irreparable HO-cut**
812 ***HA-YRA1 WT* and *HA-yra1* mutant strains (A)** Spot test analysis on plates
813 containing SCLGg Glu 2% and SCLGg Gal 2% of confluent cultures of
814 integrated *HA-YRA1 WT* and *HA-yra1* mutants containing the HO irreparable
815 DSB. A *YRA1* WT strain without any galactose-inducible irreparable HO cut is
816 shown as control. **(B)** Protein levels of HA-Yra1 WT, HA-yra1(1-210) and HA-
817 yra1allKR expressed from copies integrated into the GA-6844 strain (25) after
818 2h in Glucose or Galactose to induce the irreparable HO cut. Yra1 proteins
819 were detected with an αHA antibody and values normalized to Pgk1 protein
820 levels. The levels of WT or mutant HA-Yra1 proteins remain quite constant
821 between the different time points Glu 2h, Gal (0.5h, 1h, 2h). Values of HA-
822 Yra1/Pgk1 are shown below the blot. One representative Western Blot is
823 shown. **(C)** Quantification of the Western blot. The average of 3 independent
824 experiments is shown with corresponding standard error of the mean. HA-
825 Yra1 protein levels were normalized to HA-Yra1 WT in Glu 2h set to 1.
826

827 **S6 Fig: Yra1 mutants have comparable HO cut efficiency in the**
828 **irreparable and repairable systems. (A)** Analysis of HO cut site levels in the
829 GA6844 strain described in (25) after 0.5h, 1h, 2h and 4h of HO
830 endonuclease induction with galactose. The genomic locus was quantified by
831 qPCR (with oligos OFS2682 + OFS2683) and the level was normalized to
832 *SCR1*. The average of 6 independent experiments is shown with
833 corresponding standard error of the mean. **(B)** Analysis of HO cut site levels
834 in the *HA-YRA1 WT* and *HA-yra1* mutants integrated in GA6844 strain
835 described in (25) after 2h of HO endonuclease induction with galactose or 2h
836 in Glucose (no HO induction). The genomic locus was quantified by qPCR
837 (with oligos OFS2682 + OFS2683) and the level was normalized to *SCR1*.
838 The average of 3 independent experiments is shown with corresponding
839 standard error of the mean. **(C)** Analysis of HO cut site levels in *HA-YRA1 WT*
840 (WT), *HA-yra1(1-210)*, *HA-yra1allKR* and No-Tag strains treated with
841 Galactose 2% (cut induction) or not (control) for 2h. The genomic locus was
842 quantified by qPCR using oligos next to the HO site (OFS4188-OFS4179) and
843 the level was normalized to *SCR1*. The HO cut levels in galactose are
844 expressed relative to those in glucose. The average of 2 independent
845 experiments is shown with corresponding standard error of the mean.
846
847 **S7 Fig: Levels of Rad51 in *HA-YRA1 WT* and *HA-yra1* mutant strains.**
848 Protein levels of Yra1 (αHA), Pgk1 (αPgk1), Rad51 (αRad51) in *HA-YRA1*
849 *WT*, *HA-yra1(1-210)* and *HA-yra1allKR* analyzed by Western blot. The right
850 graph shows the Western blot quantification of the ratio of Rad51/Pgk1 of
851 three independent experiments with relative standard error of the mean.

852 The quantifications were performed using Lycor Software. Rad51 protein
853 levels were normalized to those in *HA-YRA1 WT* that were set to 1.

Fig 1

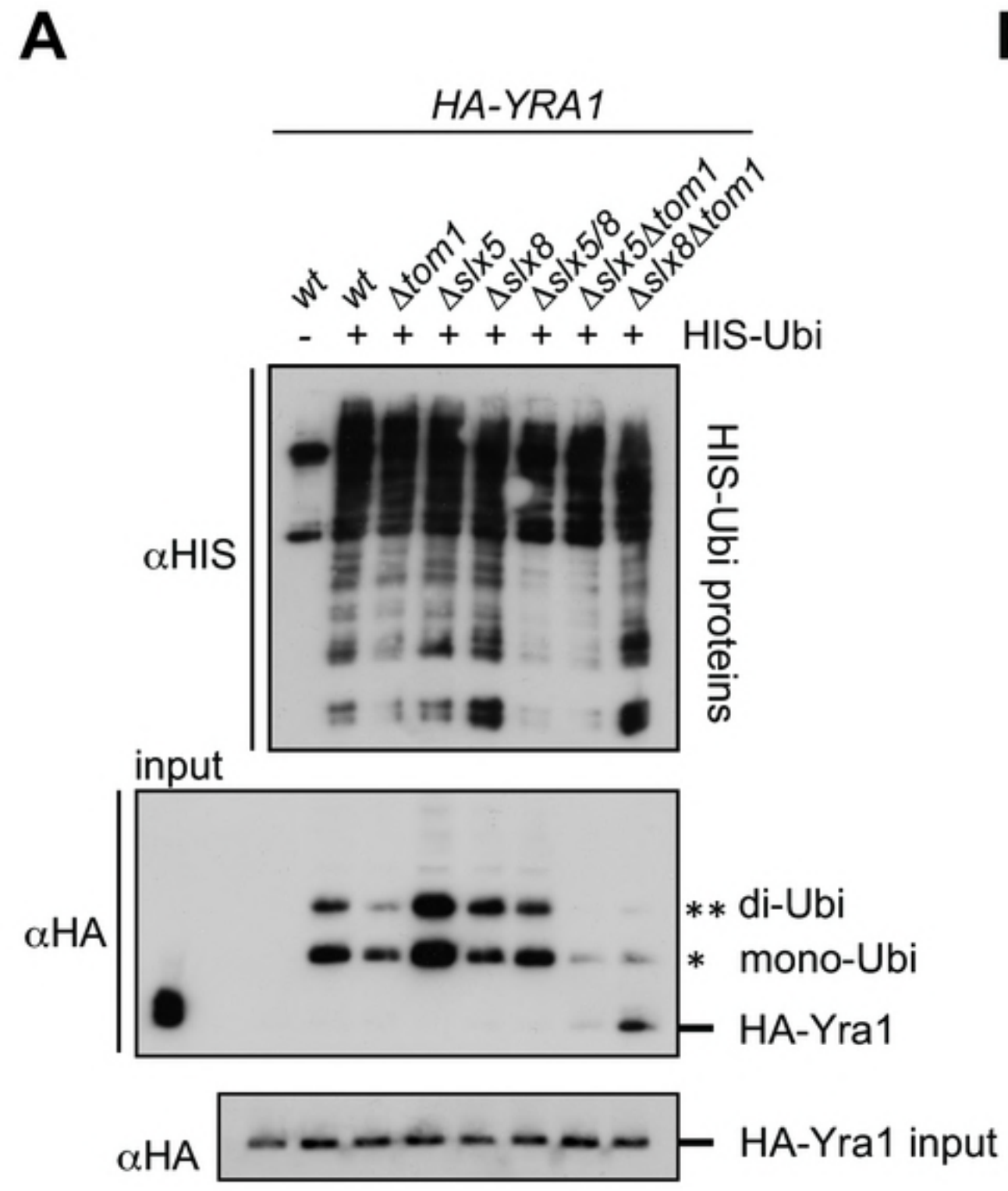
A
HA-YRA1
wt
wt
Δtom1
Δslx5
Δslx8
Δslx5/8
Δslx5Δtom1
Δslx8Δtom1
- + + + + + + + HIS-Ubi
αHIS
HIS-Ubi proteins
input
αHA
** di-Ubi
* mono-Ubi
HA-Yra1
αHA
HA-Yra1 input

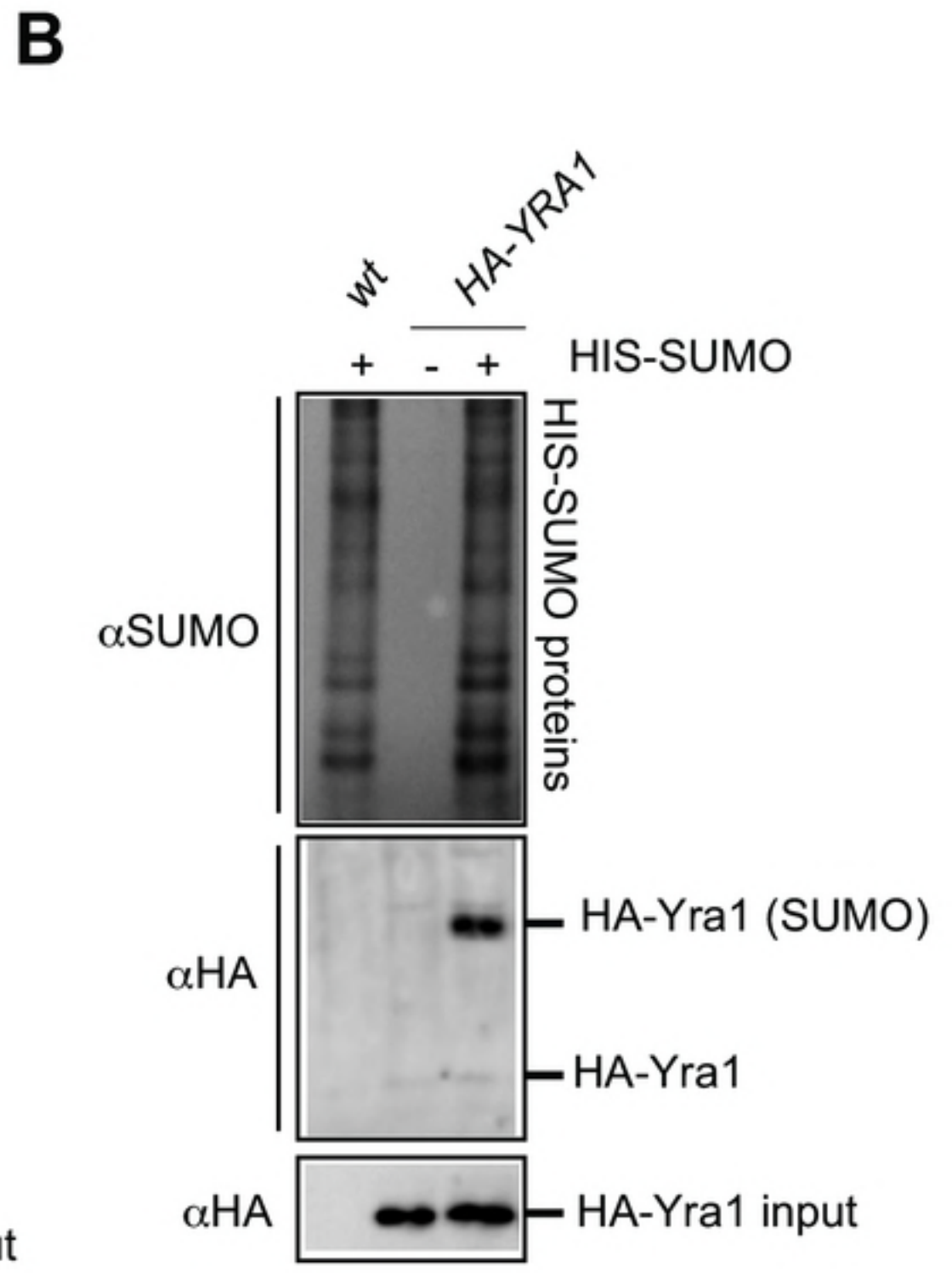
B
wt
HA-YRA1
+ - + HIS-SUMO
αSUMO
HIS-SUMO proteins
αHA
HA-Yra1 (SUMO)
HA-Yra1
αHA
HA-Yra1 input

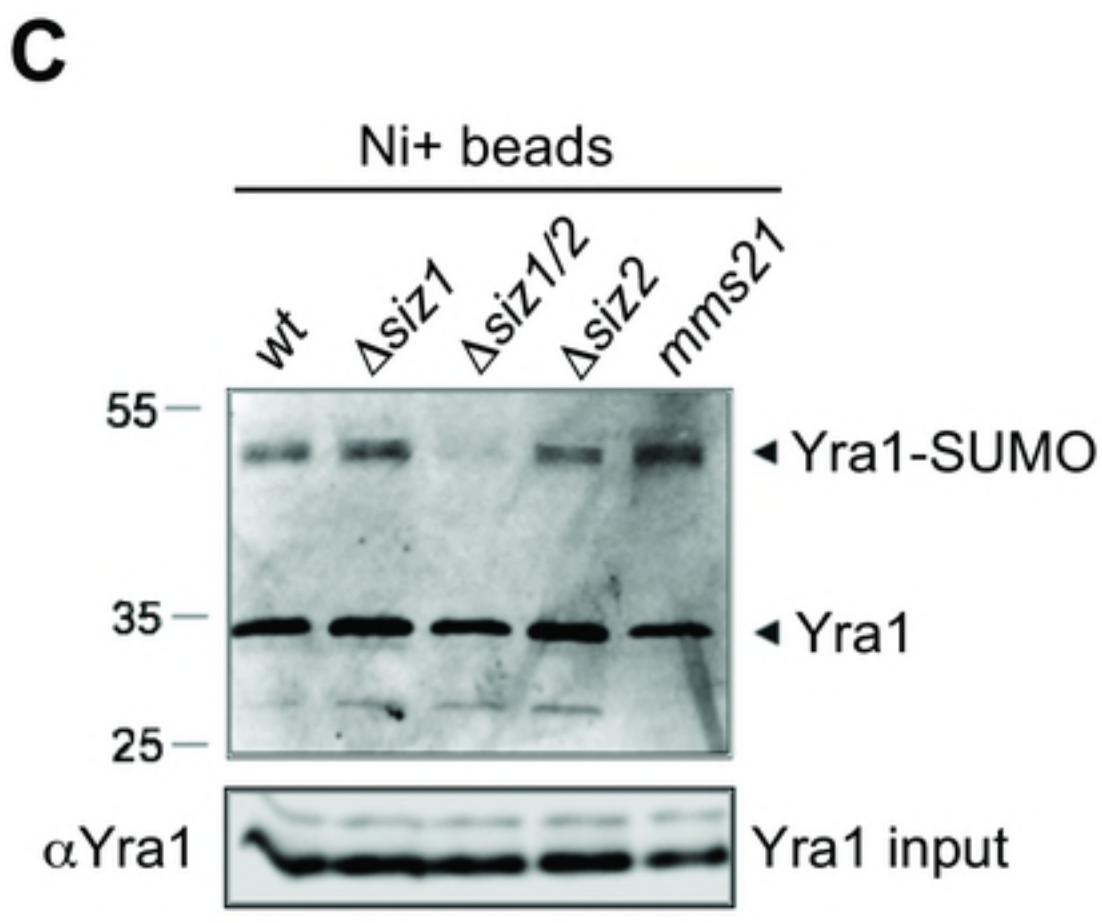
C
Ni+ beads
wt
Δsiz1
Δsiz1/2
Δsiz2
mms21
55
35
25
Yra1-SUMO
Yra1
αYra1
Yra1 input

Fig 2

A

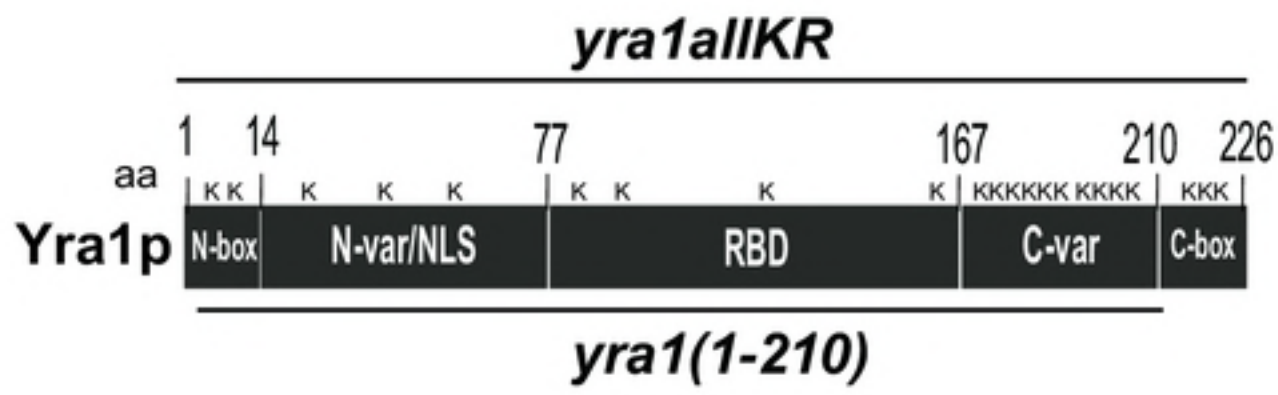
yra1allKR
aa
1
14
77
167
210
226
Yra1p
N-box
N-var/NLS
RBD
C-var
C-box
yra1(1-210)

B

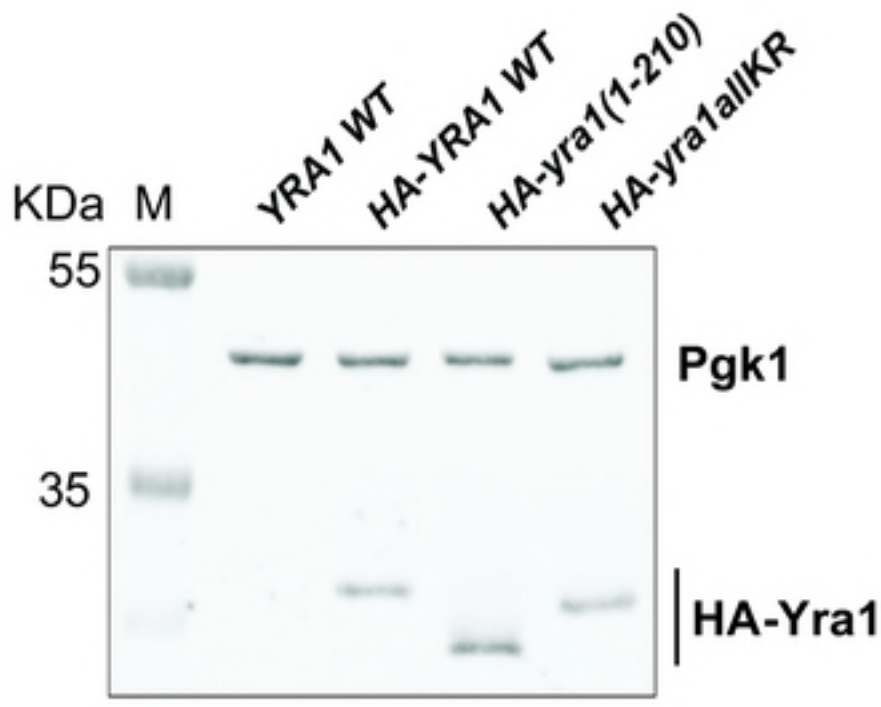
KDa
M
YRA1 WT
HA-YRA1 WT
HA-yra1(1-210)
HA-yra1allKR
55
35
Pgk1
HA-Yra1

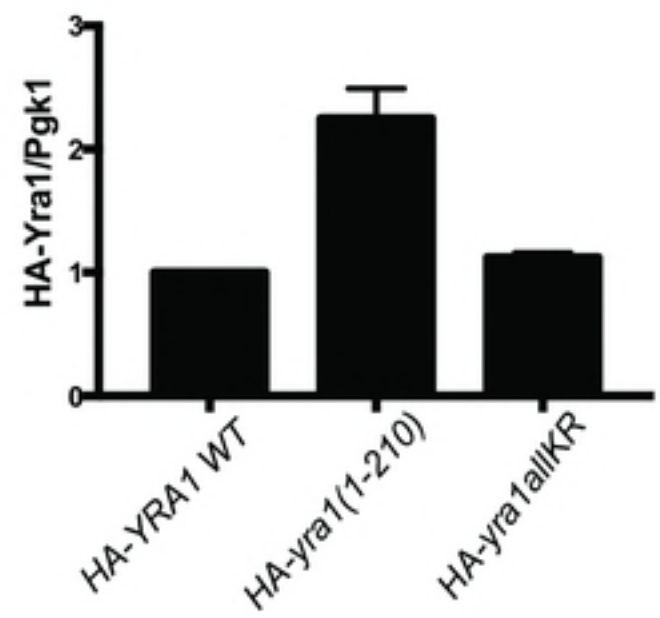
HA-Yra1/Pgk1
0
1
2
3
HA-YRA1 WT
HA-yra1(1-210)
HA-yra1allKR

C

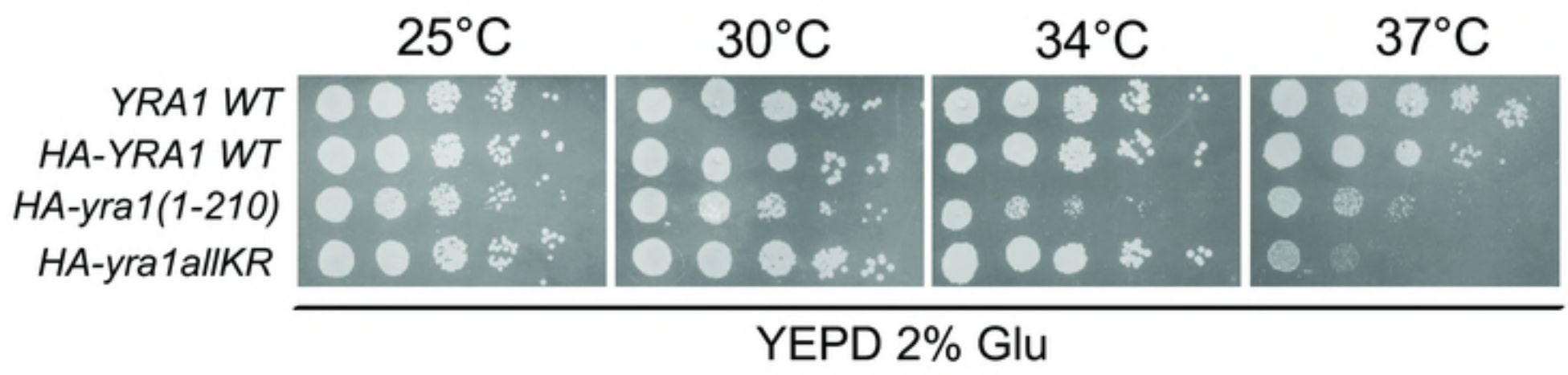
25°C
30°C
34°C
37°C
YRA1 WT
HA-YRA1 WT
HA-yra1(1-210)
HA-yra1allKR
YEPD 2% Glu

D

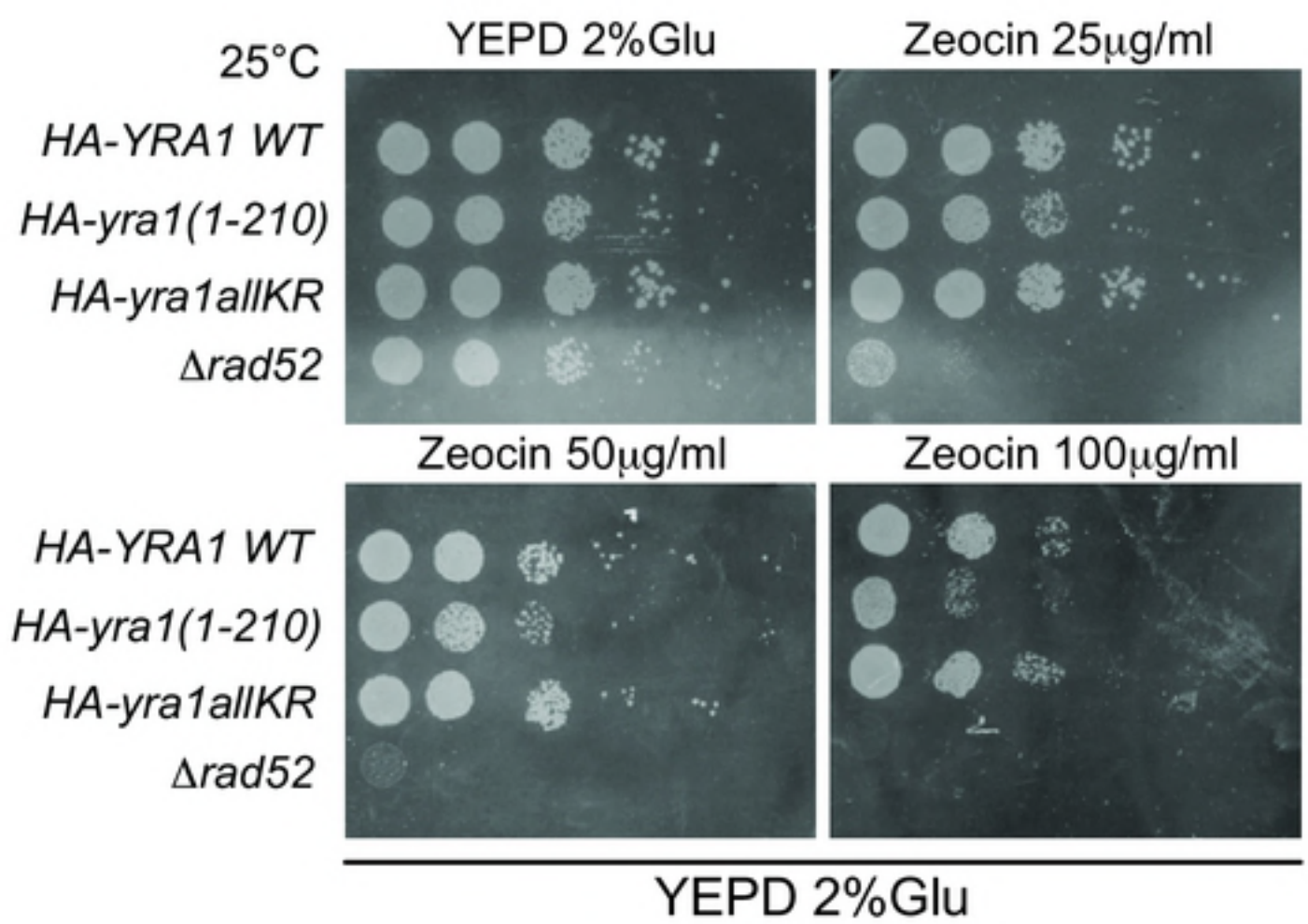
25°C
YEPD 2%Glu
Zeocin 25μg/ml
HA-YRA1 WT
HA-yra1(1-210)
HA-yra1allKR
Δrad52
Zeocin 50μg/ml
Zeocin 100μg/ml
HA-YRA1 WT
HA-yra1(1-210)
HA-yra1allKR
Δrad52
YEPD 2%Glu

Fig 3

A

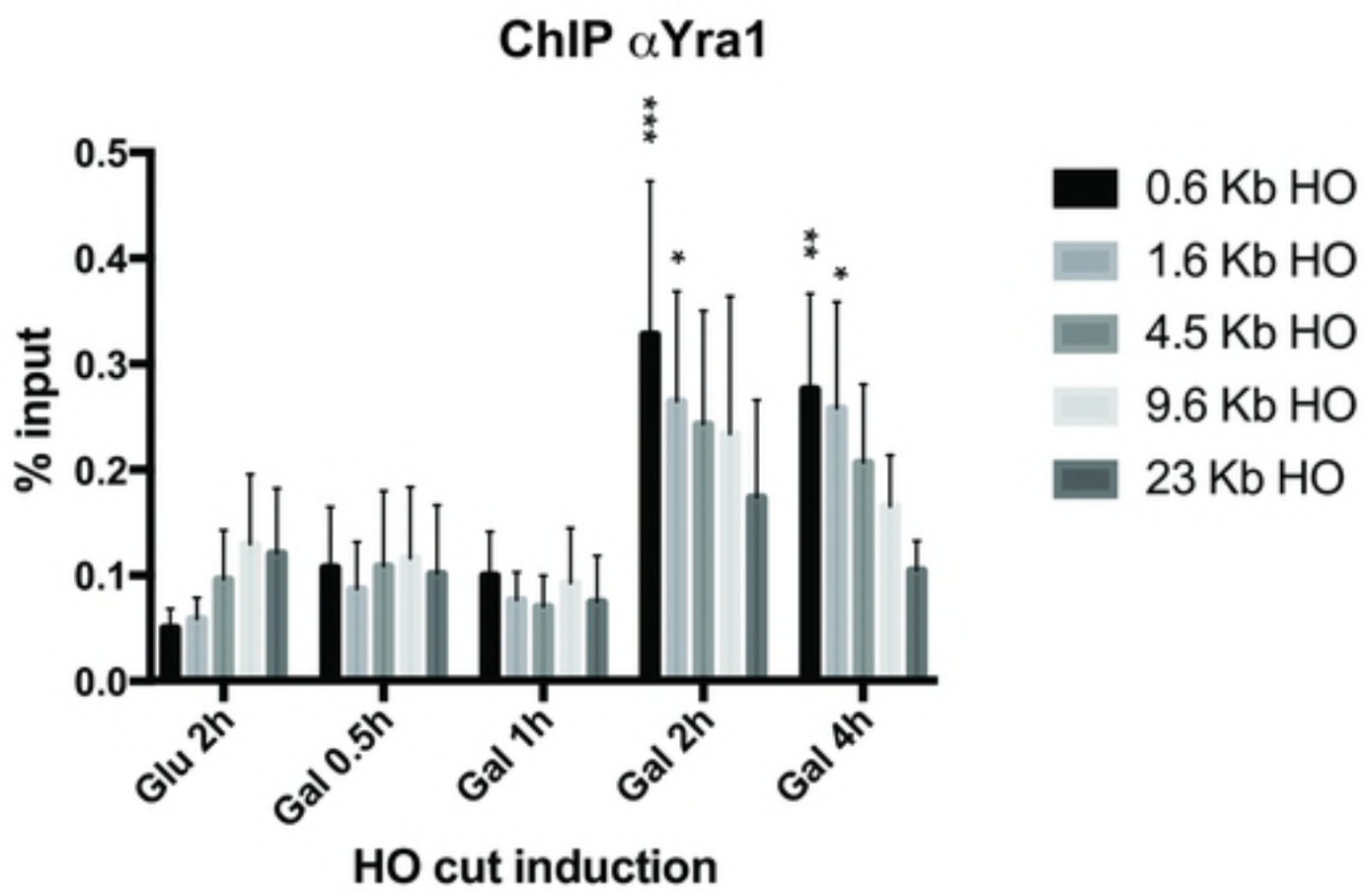
ChIP αYra1
% input
0.5
0.4
0.3
0.2
0.1
0.0
***
*
**
*
Glu 2h
Gal 0.5h
Gal 1h
Gal 2h
Gal 4h
HO cut induction
0.6 Kb HO
1.6 Kb HO
4.5 Kb HO
9.6 Kb HO
23 Kb HO

B

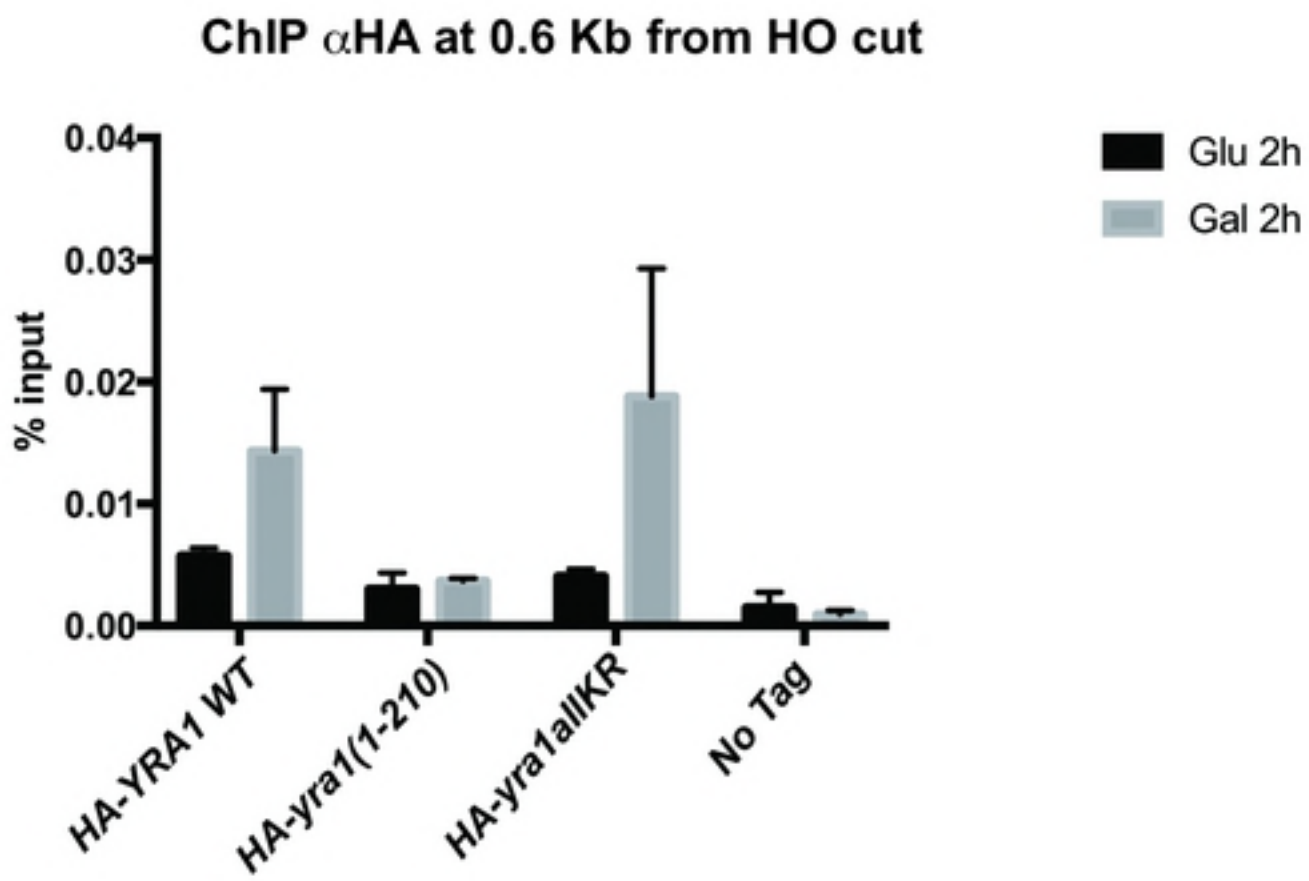
ChIP αHA at 0.6 Kb from HO cut
% input
0.04
0.03
0.02
0.01
0.00
HA-YRA1 WT
HA-yra1(1-210)
HA-yra1allKR
No Tag
Glu 2h
Gal 2h

C

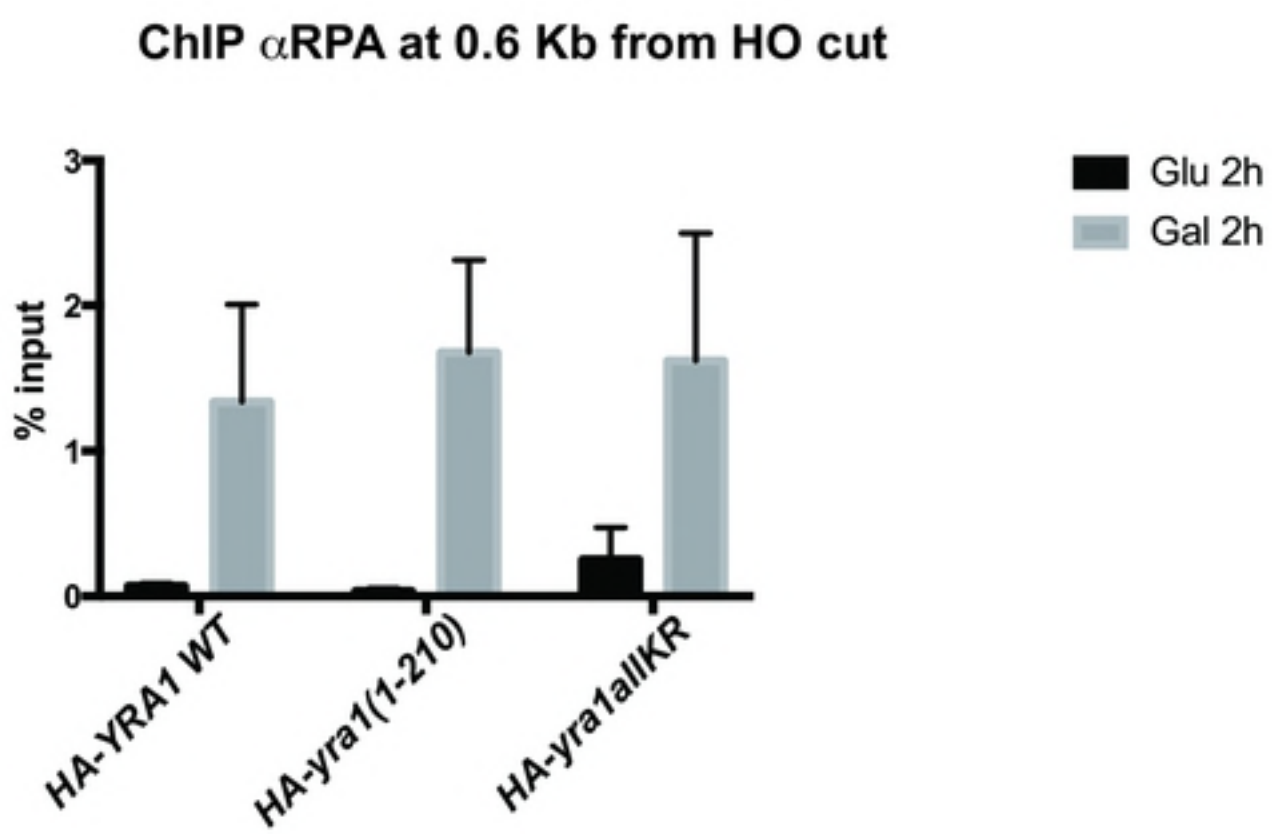
ChIP αRPA at 0.6 Kb from HO cut
% input
3
2
1
0
HA-YRA1 WT
HA-yra1(1-210)
HA-yra1allKR
Glu 2h
Gal 2h

Fig 4

A

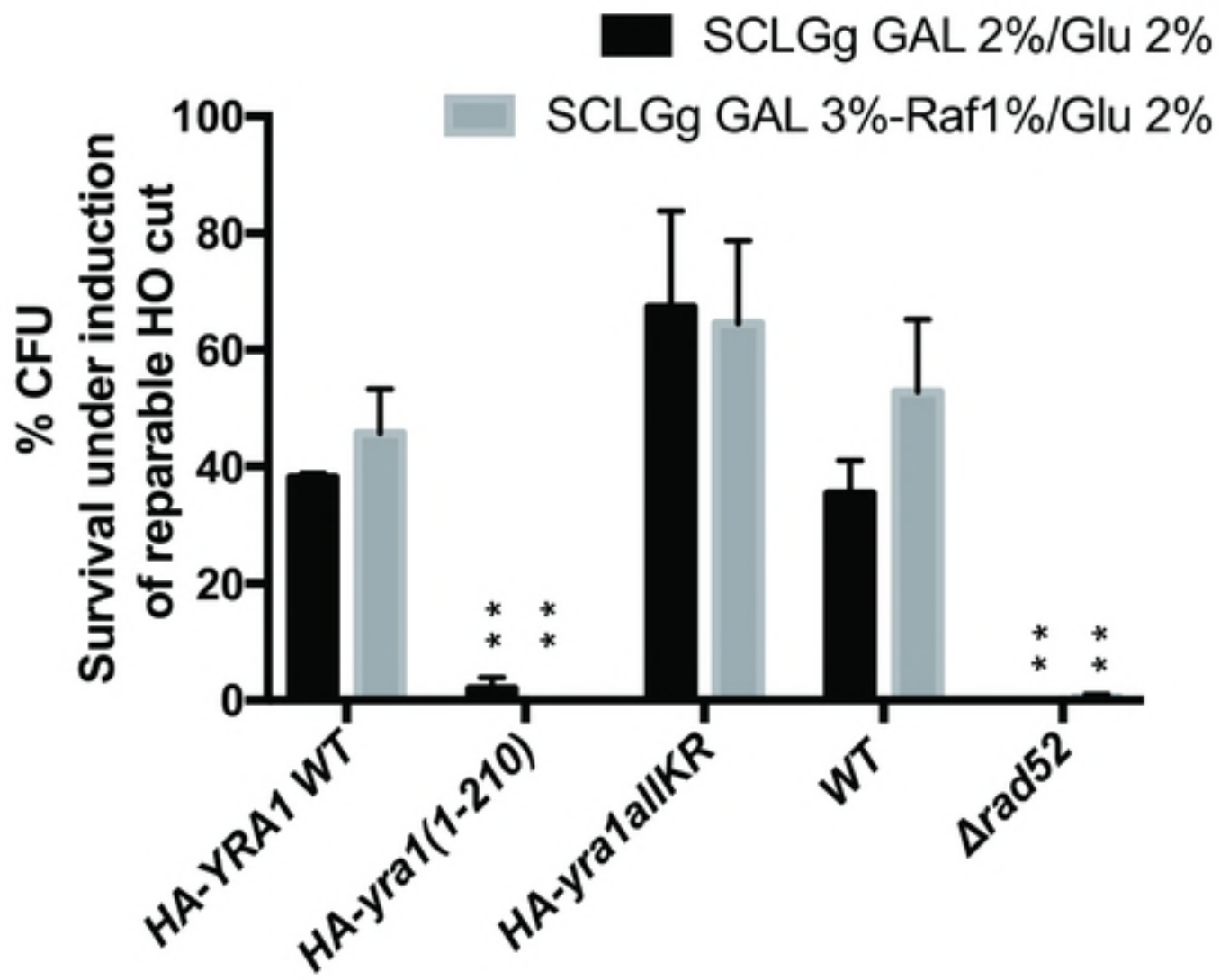
SCLGg GAL 2%/Glu 2%
SCLGg GAL 3%-Raf1%/Glu 2%
% CFU
Survival under induction
of reparable HO cut
100
80
60
40
20
0
HA-YRA1 WT
HA-yra1(1-210)
HA-yra1allKR
WT
Δrad52

B

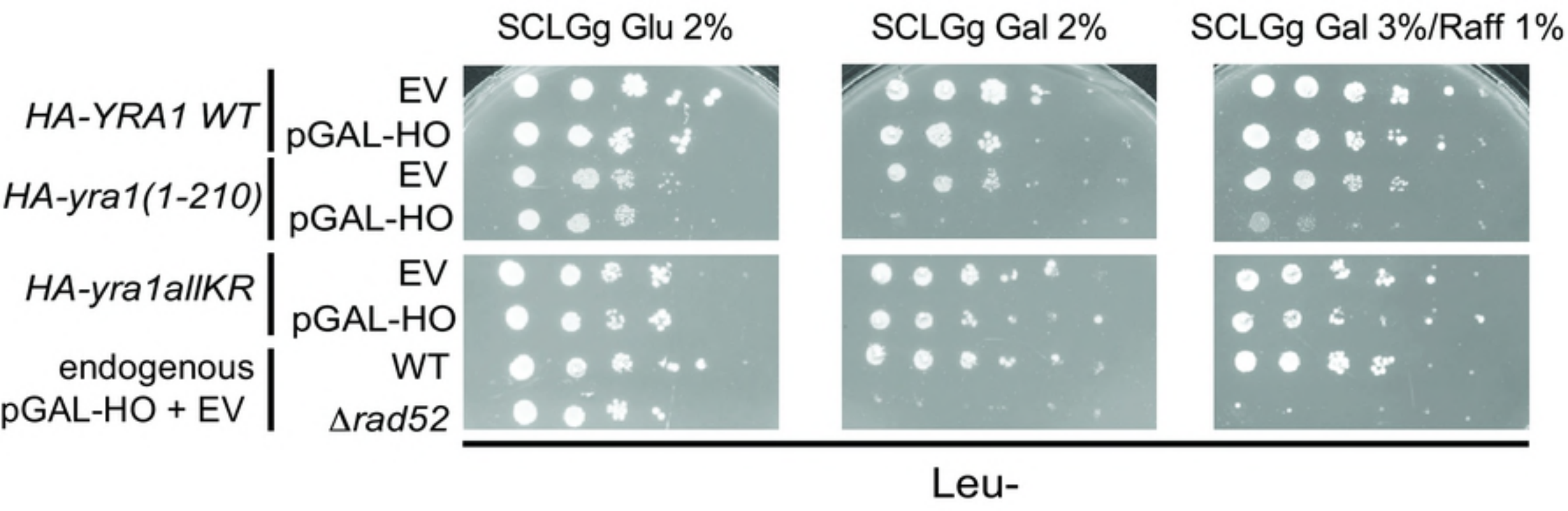
SCLGg Glu 2%
SCLGg Gal 2%
SCLGg Gal 3%/Raff 1%
HA-YRA1 WT
EV
pGAL-HO
HA-yra1(1-210)
EV
pGAL-HO
HA-yra1allKR
EV
pGAL-HO
endogenous
pGAL-HO + EV
WT
Δrad52
Leu-